Journal of Neuroinflammation

RESEARCH

Open Access

Differential effect of an evolving amyloid and tau pathology on brain phospholipids and bioactive lipid mediators in rat models of Alzheimer-like pathology

Sonia Do Carmo[1*], Marie-Audrey I. Kautzmann[2], Surjyadipta Bhattacharjee[2], Bokkyoo Jun[2], Carolyn Steinberg[1], Joshua T. Emmerson[1], Janice C. Malcolm[3], Quentin Bonomo[4], Nicolas G. Bazan[1,2*] and A. Claudio Cuello[1,3,4,5*]

Abstract

Background Brain inflammation contributes significantly to the pathophysiology of Alzheimer's disease, and it is manifested by glial cell activation, increased production of cytokines/chemokines, and a shift in lipid mediators from a pro-homeostatic to a pro-inflammatory profile. However, whether the production of bioactive lipid mediators is affected at earlier stages, prior to the deposition of Aβ plaques and tau hyperphosphorylation, is unknown. The differential contribution of an evolving amyloid and tau pathology on the composition and abundance of membrane phospholipids and bioactive lipid mediators also remains unresolved.

Methods In this study, we examined the cortical levels of DHA- and AA-derived bioactive lipid mediators and of membrane phospholipids by liquid chromatography with tandem mass spectrometry in transgenic rat models of the Alzheimer's-like amyloid and tau pathologies at early and advanced pathological stages.

Results Our findings revealed a complex balance between pro-inflammatory and pro-resolving processes in which tau pathology has a more pronounced effect compared to amyloid pathology. At stages preceding tau misfolding and aggregation, there was an increase in pro-resolving lipid mediators (RVD6 and NPD1), DHA-containing phospholipids and IFN-γ levels. However, in advanced tau pathology displaying NFT-like inclusions, neuronal death, glial activation and cognitive deficits, there was an increase in cytokine and PGD2, PGE2, and PGF2α generation accompanied by a drop in IFN-γ levels. This pathology also resulted in a marked increase in AA-containing phospholipids. In comparison, pre-plaque amyloid pathology already presented high levels of cytokines and AA-containing phospholipids together with elevated RVD6 and NPD1 levels. Finally, Aβ plaque deposition was accompanied by a modest increase in prostaglandins, increased AA-containing phospholipids and reduced DHA-containing phospholipids.

*Correspondence:
Sonia Do Carmo
sonia.docarmo@mcgill.ca
Nicolas G. Bazan
NBazan@lsuhsc.edu
A. Claudio Cuello
claudio.cuello@mcgill.ca

Full list of author information is available at the end of the article

Conclusions Our findings suggest a dynamic trajectory of inflammatory and lipid mediators in the evolving amyloid and tau pathologies and support their differing roles on membrane properties and, consequentially, on signal transduction.

Keywords Alzheimer's disease, Amyloid pathology, Tauopathy, Transgenic rat, Lipidomics, Brain phospholipids, Bioactive lipid mediators, Neuroinflammation

Background

Alzheimer's disease (AD), the most common form of dementia, is characterized by a progressive and irreversible loss of cognitive functions, resulting in the inability to carry out daily activities. AD pathology develops for decades before its clinical presentation [1], at which point currently available therapies are ineffective. In addition to extracellular amyloid beta (Aβ) plaques and intraneuronal neurofibrillary tangles (NFTs) composed of abnormally phosphorylated and aggregated tau, neuroinflammation is increasingly considered as the third core pathological feature of AD. This concept is supported by genome-wide association studies indicating that immune-related genes are significant risk factors for AD [2–7]. The trigger, function, and trajectory of AD-related brain inflammation remain controversial. It is evident that neuroinflammation contributes significantly to the development and progression of AD, aggravating both Aβ and tau pathologies [4, 8, 9]. Evidence gathered from human and animal studies also suggests that inflammation is a dynamic process differing at the early and late stages of AD [10] (reviewed in [11]). Neuroinflammatory molecules also accumulate in the brain in healthy aging [12, 13]. Furthermore, epidemiological studies have shown that cognitively intact individuals receiving sustained nonsteroidal anti-inflammatory drugs (NSAIDs) had approximately 50% lower incidence of clinical AD than the general population [14]. This finding promoted AD anti-inflammatory therapy, which has proved ineffective after clinical presentation [14–19]. This highlights the need for a better understanding of the driving forces behind the constantly evolving inflammatory process.

As it is well-established, transient, self-limiting neuroinflammation represents the brain's natural response to invading pathogens and neuronal injury, and it is usually neuroprotective by contributing to the clearance of debris, sustaining synaptic plasticity, and promoting neurogenesis [20, 21]. However, when the active resolution mechanisms fail, there is a self-perpetuating activation of inflammatory processes, leading to chronic neuroinflammation and ultimately progressing into a neurodegenerative state. The resolution of inflammation is, in part, controlled by a switch in the production of lipid mediators from a pro-inflammatory to a pro-resolving class [22]. Lipid mediators are synthesized from cell membrane phospholipids through the action of several key enzymes, including phospholipase A2 (PLA2). In response to inflammatory stimuli, PLA2 releases omega-6 (linoleic acid (LA) and arachidonic acid (AA)) and omega-3 (eicosapentaenoic acid (EPA) and docosahexaenoic acid (DHA)) polyunsaturated fatty acids (PUFAs) from the membrane phospholipids into the cytosol where they serve as substrates for the biosynthesis of bioactive lipid mediators through the cyclooxygenase (COX), lipoxygenase (5-LOX/15-LOX) and cytochrome P450 (CYP) enzymatic pathways [23].

Reductions in the levels of pro-resolving lipid mediators and their receptors, as well as increases in pro-inflammatory lipid mediators, have been evidenced in post-mortem brain tissue and in CSF from mild cognitive impairment (MCI) and AD patients, as well as in AD experimental models [22, 24–27]. Importantly, in CSF, specific pro-inflammatory and pro-resolving lipid mediators showed significant correlations with cognitive measures and with classical biomarkers of AD (Aβ42, tau, p-tau) as early as at subjective cognitive impairment (SCI) stages [22, 26]. However, whether the production of bioactive lipid mediators is affected at earlier stages, prior to the deposition of Aβ plaques and tau hyperphosphorylation, is unknown. The differential contribution of an evolving amyloid and tau pathology on the composition and abundance of membrane phospholipids and bioactive lipid mediators also remains unresolved. To shed some light on these questions, in this study, we examined the cortical levels of DHA- and AA-derived lipid mediators and of phospholipids in transgenic rat models of the AD-like amyloid and tau pathologies at early and advanced pathological stages.

Materials and methods

Animals

The McGill-R962-hTau (high expressor) and McGill-R955-hTau (low expressor) transgenic rat lines overexpress the coding region of the 2N4R isoform of human tau (MAPT) bearing the P301S mutation causative of FTDP-17 [28], under the control of the mouse CAMKIIα promoter cassette, which directs expression to neurons of the forebrain, as described previously [29–31]. Both lines are derived from the founders obtained following the same pronuclear injection. Heterozygous R955-hTau rats possess a milder tau pathology phenotype compared to R962-hTau (summarized in Fig. 1), in accordance with their transgene copy number (estimated to 4 and 30 insertions, respectively). The McGill-R-Thy1-APP

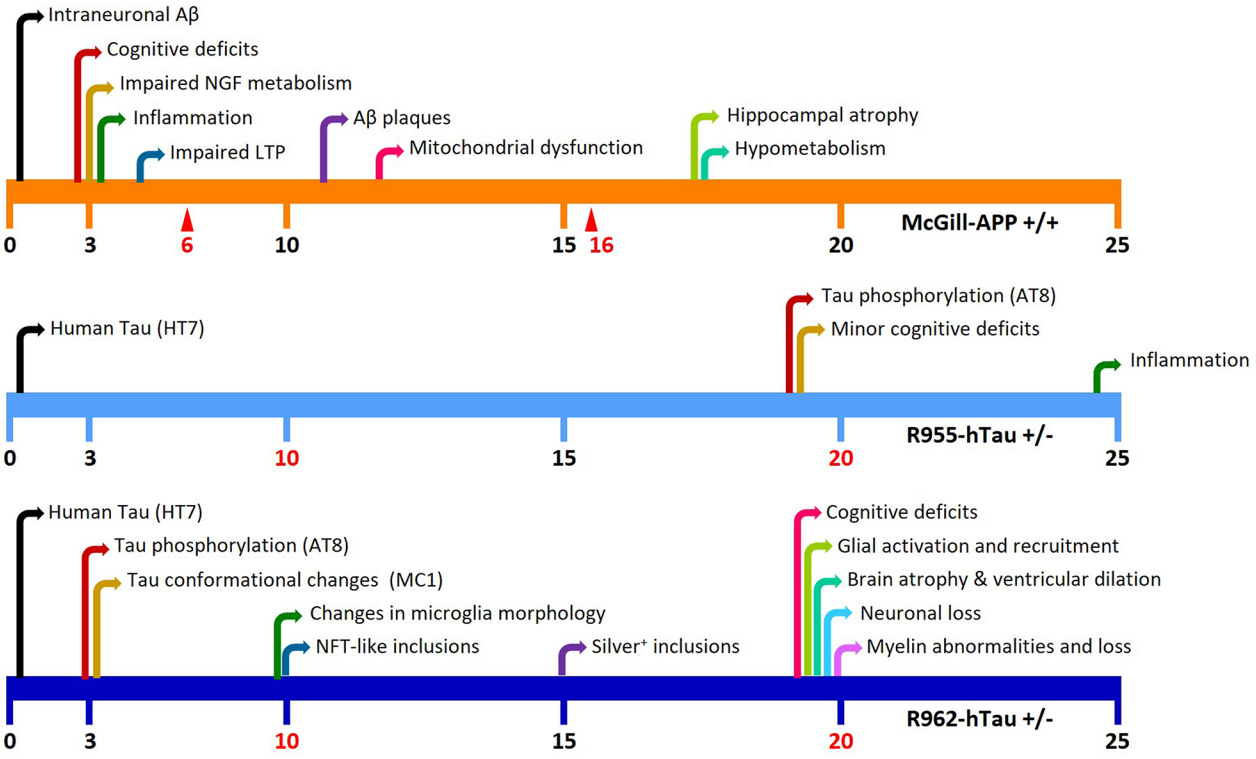

Fig. 1 Schematic representation of the evolution of the amyloid and tau pathologies in the 3 lines of transgenic rats applied in this study. Note the accelerated tau pathology in R962- compared to the R955-hTau line. The time-points studied are indicated with red arrows in McGill-APP+/+ rats (6 and 16 months) and with red font in hTau rats (10 and 20 months)

transgenic rat line overexpresses the human APP751 isoform with the Swedish and Indiana mutations under the control of the murine Thy1 promoter [32]. Rats were housed in pairs in temperature and humidity regulated rooms under a 12-hour light/dark cycle and were given standard chow and water *ad libitum*. All animal procedures were carried out under strict adherence to the guidelines set down by the Canadian Council of Animal Care and were approved by the Animal Care Committee of McGill University.

Experimental design

We examined (sex-balanced) cohorts of heterozygous male and female R955-hTau and R962-hTau transgenic rats and their corresponding wild-type (wt) littermates at 10 and 20 months of age, representing progressive stages of tau pathology as described in the results section and in Fig. 1 (n=3–5 rats per genotype at each age). We also analyzed homozygous male and female McGill-APP rats and their wt littermates at 6 and 16 months of age, representing pre- and post-plaque amyloid pathology stages, respectively (n=3–5 rats per genotype at each age).

Tissue collection

Rats were deeply anesthetized with 1% pentobarbital (Equithesin) and then perfused transcardially with cold physiological saline prior to harvesting the brains. One hemisphere was post-fixed in 4% paraformaldehyde (PFA) in 0.1 M phosphate buffer for 24 h followed by saturation in 30% sucrose in 0.1 M phosphate buffer. Coronal Sect. (40 µm-thick) were cut using a freezing microtome (Leica SM 2000R, Germany) and stored at -20 °C in cryoprotectant solution (1.1 M sucrose, 37.5% ethylene glycol in phosphate buffer saline (PBS)). The other hemisphere was macrodissected, and the cerebral cortex was snap-frozen on dry ice and stored at -80 °C.

Immunohistochemistry

To examine total human tau distributions, we applied immunoenzymatic procedures as previously described [29–31]. Brain sections were quenched in 3% hydrogen peroxide and 10% methanol in tris-buffered saline (TBS) for 30 min. Tissue was then blocked in 10% normal goat serum (NGS) in TBS containing 0.1% Triton (TBS-T) for 1 h at room temperature. After blocking non-specific antibody binding, sections were incubated with the primary antibody anti-human Tau (HT7, 1:1200, ThermoFisher, USA) in 10% NGS in TBS-T overnight at 4°C. After washing, sections were incubated with a goat anti-mouse-IgG (1:100, MP Biomedicals, USA) in 10% NGS in TBS-T for 1 h at room temperature. Signal amplification was performed with anti-horseradish peroxidase (HRP)

monoclonal antibody (1:30) pre-incubated with 5 ug/mL HRP (MAP kit; MediMabs, Canada). Stainings were developed with 0.06% 3,3'-diaminobenzidine. Sections were mounted onto gelatin-coated slides, dried overnight, and then dehydrated in increasing concentrations of ethanol, delipidated in xylene and coverslipped with Entellan mounting media (EM Science, USA).

A similar protocol was applied to examine levels of intracellular amyloid beta (Aβ) peptides, as previously described [33]. However, PBS was used as a buffer instead of TBS at all steps. After quenching and blocking in 10% NGS in PBS-T, sections were incubated with the primary antibody anti-Aβ (McSA1, 1:4000; Medimabs, Canada) (Grant et al. 2000) in 5% NGS overnight at 4 °C. Then, sections were incubated with a goat anti-mouse-IgG (1:100, MP Biomedicals, USA) in 5% NGS in PBS-T for 1 h at room temperature. The following steps were performed as described above.

Images were acquired using an Axioplan 2 imaging microscope (Carl Zeiss, Germany) equipped with an Axiocam 506 color digital camera (Zeiss) and running Zen Blue software (Zeiss).

Immunofluorescence

When available, additional animals were included to include the statistical power of the analyses. Briefly, 40-µm-thick free floating brain Sect. (2 per animal) were incubated 30 min at 80 °C in 10 mM citrate buffer (pH 6.0) for antigen retrieval, then cooled for 20 min at room temperature. Sections were then washed with PBS and incubated with 50% ethanol to permeabilize cell membrane. Hereafter PBS-T was used for all washes, and incubations were all performed at room temperature, if not otherwise specified. Sections were washed and non-specific binding sites were blocked by incubating 1 h with 10% NGS in PBS-T. Sections were then incubated overnight at 4 °C with rabbit polyclonal COX-2 antibody (1:100, Invitrogen) and mouse monoclonal AT8 antibody (1:200, Invitrogen) in 5% NGS-PBS-T. The following day, sections were washed and incubated with goat anti-rabbit Alexa 488 and goat anti-mouse Alexa 568 secondary antibody in 5% NGS-PBS-T for 2 h. Sections were then washed and incubated with 0.3% Sudan Black in 70% ethanol for 5 min to reduce background autofluorescence. After washing with PBS-T then PBS, sections were mounted on gelatin-coated slides, coverslipped with Aqua-Poly/Mount (Polysciences) and kept at 4 °C in the dark. Negative control experiments including application of secondary antibody alone (no primary) and primary alone (no secondary) were performed. Omission of primary antibodies resulted in no detectable fluorescent staining. Images were acquired as described above. Images from 2 sections per animal were acquired for the lamina I-III of the parietal cortex (two image regions) and the CA1 (two image regions). To allow quantitative comparisons, images were acquired with the same microscope settings, adjusted specifically for each marker assessed. For image analyses, custom, automated ImageJ macros were created for each target investigated. We calculated COX-2 immunoreactivity (green) as the total mean grey value (optical density).

Western blotting of cortical homogenates

Cortical tissue (20 mg) was homogenized by sonication in 8 volumes of cell lysis buffer (20 mM Tris-HCL pH 7.5, 150 mM NaCl, 1 mM Na_2EDTA, 1 mM EGTA, 1% Triton, 2.5 mM sodium pyrophosphate, 1 mM Na_3VO_4, 1 µg/ml of leupeptin, 1 mM β-glycerophosphate; Cell Signaling Technologies) containing protease inhibitors (cOmplete™ Protease Inhibitor Cocktail, Roche Applied Sciences). The homogenates were centrifuged at 13,000 rpm for 45 min at 4 °C and the supernatants were kept at -80 °C. Protein concentration was measured using a modified Lowry assay (DC Assay, Bio-Rad laboratories Inc). Equal amounts of sample (20 µg) were diluted in loading buffer (10% glycerol, 0.08 M SDS, 5% β-mercaptoethanol and 0.05 M Tris pH 6.8), heated at 90 °C for 5 min, and run on a 12% polyacrylamide gel at 100 V for 2 h. Proteins were transferred onto a methanol-activated polyvinylidene difluoride membrane at 0.3 A for 1 h. After blocking in 5% non-fat milk in TBS-T for 1 h, membranes were incubated with primary antibodies directed against Tau (Tau5) (MAB361, Millipore; 1:750), NfL (ab7255, Abcam, 1:5000) or βIII-tubulin (G712A, Promega; 1:1000), in 5% non-fat milk in TBS-T overnight at 4 °C. Membranes were washed and incubated with a species-specific secondary antibody for 1 h at room temperature. Immunoreactive bands were revealed using enhanced chemiluminescence substrate (PerkinElmer, Inc.) in an Amersham Imager 600. Optical density of each band was determined using the ImageLab software. All values were normalized by GAPDH and expressed as relative values compared to wt. Each experiment was repeated a minimum of two times.

Quantification of Aβ42 and cytokines

Cortical tissue (40 mg) was homogenized by sonication in 8 volumes of Tris-buffered saline buffer (150 mM NaCl, 50 mM Tris HCl, 5 mM EDTA, pH 7.6) containing protease inhibitors (cOmplete Mini Protease Inhibitor Cocktail, Roche). Homogenates were ultracentrifuged at 100,000 g for 1 h (soluble fraction). The pellets were resuspended in 5 volumes of guanidine buffer (5 M guanidine HCl, 50 mM Tris HCl, pH 8.0), sonicated, and incubated for 3 h. The supernatants (insoluble fraction) were collected after ultracentrifugation at 100,000 g for 1 h.

Levels of human Aβ42 were assayed in soluble and insoluble fractions in duplicate using the MesoScale Discovery V-plex Aβ Peptide Panel 1(6E10) kit and the SECTOR Imager 6000 (MesoScale Discovery, Rockville, MD). Soluble cortical fractions were pre-diluted to 4 ug protein/ul and assayed at a 1:2 dilution in Diluent 35. Insoluble cortical fractions were pre-diluted to 10 ug protein/ul and assayed at a 1:50 dilution. Analyte concentrations were calculated in reference to calibrators for each individual analyte using the MSD Discovery Workbench software v. 4.0 (Meso Scale Discovery). Values were normalized to total protein input and expressed as pg Aβ peptide/mg protein. The dynamic range for Aβ38 was 8.12–12,200 pg/ml, for Aβ40 4.89–15,300 pg/ml, and for Aβ42 0.328–1710 pg/ml.

Levels of cytokines and chemokines were determined in soluble fractions pre-diluted to 4 µg protein/ul and assayed at a 1:2 dilution in Diluent 42, in duplicate. Levels of 9 cytokines (IFN-γ, IL-1β, IL-4, IL-5, IL-6, KC/GRO, IL-10, IL-13, TNF-α) were measured using the MesoScale Discovery Proinflammatory Panel 2 (rat) kit. Cytokine concentrations were calculated from a standard curve generated by the MSD Discovery Workbench software v. 4.0. Values were normalized to total protein input and expressed as pg cytokine/mg protein.

Lipid extraction

Each cortical sample was homogenized with 3 ml MeOH and added with 9 ml CHCl3. An internal standard mixture of deuterium-labeled lipids (AA-d8, PGD_2-d4, EPA-d5, 15HETE-d8, and LTB_4-d4) was added to each sample. The samples were sonicated in a water bath for 30 min, and then stored at -80 °C. The next day, the samples were centrifuged at 4200 × g for 30 min, and the supernatants collected in a new tube. The pellets were washed with CHCl3/MeOH (2:1) and centrifuged. The supernatants from both centrifugations were combined. Two ml of distilled water, pH 3.5, were added to the combined supernatants, vortexed, and centrifuged, revealing two layers. The lower phase was dried under N_2 gas stream, resuspended in 200 µl MeOH, and transferred to MS vials. The sample was resuspended with 200ul MeOH and transferred to MS vial. Samples were dried under N2 and then resuspended with 30ul MeOH: H2O = 1:1 solvent.

LC-MS/MS

Xevo TQ-S equipped with Acquity I Class UPLC (Waters Corporation, Milford, MA) was used for lipidomics. Analysis of fatty acids and their derivatives was performed using a CORTECS 2.7 µm 4.6×100 mm C18 Column (Waters Corporation, Milford, MA). 45% of solvent A (H_2O + 0.01% acetic acid) and 55% of solvent B (MeOH + 0.01% acetic acid) with 0.4 ml/min flow was used initially and gradient to 15% of A for the first 10 min, then gradient to 2% of solvent A at 18 min. 2% of solvent A ran till 25 min, and gradient back to 45% of A for re-equilibration till 30 min. The capillary voltage was −2.5 kV, desolvation temperature at 600 C, desolvation gas flow at 1100 L/Hr, cone gas at 150 L/Hr, and nebulizer pressure at 7.0 Bar with the source temperature at 150°C. MassLynx 4.1 software was used for the operation and recording of the data. Lipid standards (Cayman, Ann Arbor, MI, USA) were used for tuning and optimization, as well as to create calibration curves for each compound. MS data were analyzed and calculated with Excel.

Analysis of phospholipids was performed using an Acquity UPLC BEH HILIC 1.7 µm 2.1×100 mm Column (Waters Corporation, Milford, MA) with solvent A (acetonitrile: water = 1:1, 10mM ammonium acetate pH 8.3) and solvent B (acetonitrile: water = 95:5, 10mM ammonium acetate pH 8.3) as mobile phase. The solvent B (100%) ran for the first 5 min isocratically, then gradient to 20% solvent A at 13 min and 65% of A at 13.5 min. For 16.5 min, it ran isocratically at 65% of A. It went back to 100% of B to 20 min for equilibration. The capillary voltage was 2.5 kV, desolvation temperature at 550 C, desolvation gas flow at 800 L/Hr, cone gas at 150 L/Hr, and nebulizer pressure at 7.0 Bar with the source temperature at 120 C. Phospholipid molecular species were calculated as % of the total amount in each sample.

Statistical analysis

Statistical analyses were performed using the software GraphPad Prism version 10 (La Jolla, USA). The D'Agostino and Pearson omnibus normality test was used to assess normal distribution of the data. Outliers were excluded using the ROUT method (Q = 1%). Graphed data is presented as mean values ± SEM. Given the small sample size, two-group comparisons were performed with the Mann-Whitney U test. Kruskal-Wallis with Dunn's post hoc tests was used for multiple comparisons. Spearman's correlation test was used to examine associations between analytes. Significance was set to $p < 0.05$.

Results

Transgenic rat models expressing mutant human APP and MAPT exhibit progressive neuropathology

To assess the differential impact of cortical tau and amyloid pathology on bioactive lipid mediators, we examined cohorts of homozygous McGill-R-Thy1-APP rats [32] and their wt littermates at 6 and 16 months of age, as well as cohorts of heterozygous McGill-R962-hTau [31] and McGill-R955-hTau [30] transgenic rats and their corresponding wt littermates at 10 and 20 months of age ($n = 3$–5 rats per genotype at each age). A summary of the phenotypes of the three transgenic lines is provided in Fig. 1.

McGill-R-Thy1-APP transgenic rats (hereafter McGill-APP rats) develop progressive AD-like amyloid pathology in the absence of tau pathology. The phenotype of McGill-APP transgenic rats has been extensively reported [34–45]. Six-month-old McGill-APP rats display intraneuronal amyloid beta (Aβ) throughout brain regions including cortical and hippocampal areas but are devoid of amyloid plaques, while extensive Aβ plaque pathology is present at 16 months, mainly in hippocampal but also in cortical areas as shown with the human Aβ-specific McSA1 antibody [46] (Fig. 2A). The Aβ plaque pathology is reflected by higher levels of soluble and foremost insoluble Aβ42, as measured by electrochemiluminescence immunoassays, in 16-month-old McGill-APP rats compared to younger rats (Fig. 2B).

McGill-R955-hTau and R962-hTau lines display an age-dependent accumulation of mutated human tau in their brain. However, heterozygous R955-hTau rats possess a milder tau pathology phenotype compared to R962-hTau (summarized in Fig. 1). Thus, as previously reported [30], 10-month-old McGill-R955-hTau+/- rats display accumulation of total human tau as shown by HT7 immunoreactivity in the subiculum and CA1, CA2 and CA3 regions of the hippocampus as well as in layers II, III of the cerebral cortices. The distribution of human tau HT7 immunoreactivity was similar but more intense in hippocampal and cortical areas at 20 months of age (Fig. 2C). In comparison, neurons of 10-month-old McGill-R962-hTau+/- rats are more heavily burdened with HT7 immunoreactivity. However, in the brain of 20-month-old McGill-R962-hTau+/- rats, in accordance with a neurodegenerative phenotype, HT7 immunoreactivity becomes less intense while a shrinkage of the hippocampal and cortical areas as well as an enlargement of the ventricles is evident (Fig. 2D). In line with the immunohistochemistry results, Western blot analyses applying

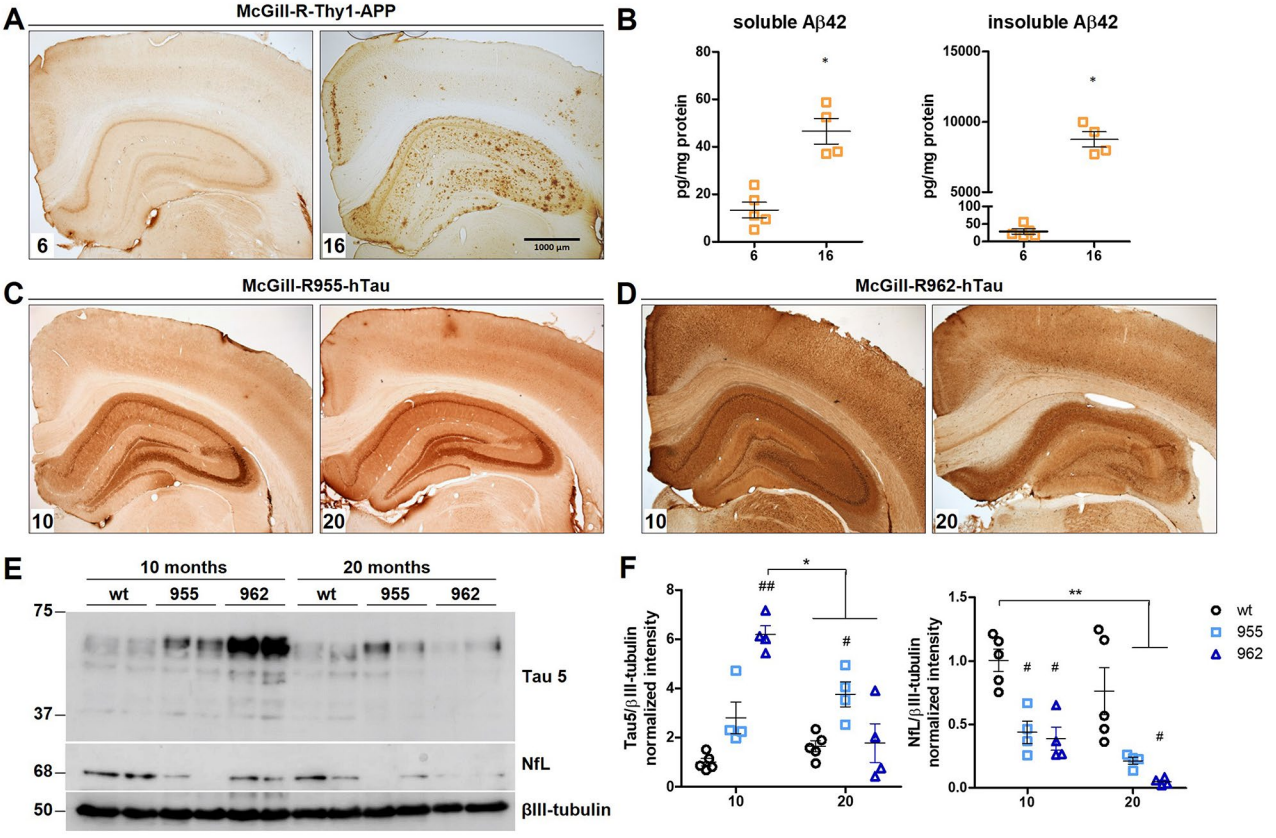

Fig. 2 Transgenic models expressing mutant human APP and MAPT exhibit progressive neuropathology. **A**. In 6-month-old McGill-R-Thy1-APP transgenic rats, human Aβ (McSA1) immunoreactivity is restricted to the intraneuronal compartment (left). By 16 months of age, human Aβ immunoreactivity has transitioned to the extracellular compartment and extensive Aβ plaque pathology is present (right). **B**. Levels of TBS-soluble and insoluble (formic-acid soluble) Aβ42 peptides were measured by ECLIA. **C-D** Both McGill-R955-hTau (**C**) and McGill-R962-hTau (**D**) transgenic rats display progressive tauopathy as assessed by HT-7 immunoreactivity. Note the hippocampal shrinkage and ventricular dilation in 20-month-old R962-hTau rats (right). Scale bar = 1000 µm. **E-F**. Levels of total tau (applying the pan-species antibody Tau5) and levels of NfL were assessed by Western blot analysis of cortical homogenates. (**F**) Quantification of the intensity of Tau5 and NfL immunoreactive bands. Values are expressed as means ± SEM ($n = 4–5$/group). Two-group comparisons were performed with the Mann-Whitney U test. Kruskal-Wallis with Dunn's post hoc tests was used for multiple comparisons. # $p < 0.05$, ## $p < 0.01$ compared to age-matched wt rats; * $p < 0.05$, ** $p < 0.01$ compared to other groups

the pan-species antibody Tau5 recognizing phosphorylated and non-phosphorylated isoforms of tau revealed that by 10 months of age, R955-hTau rats exhibit 3-fold higher levels of cortical total tau compared to wt rats and these levels rise modestly with time, reaching levels of tau ~ 4-fold higher than wt rats by 20 months (Fig. 2E-F). In comparison, the R962-hTau line produced about 3-fold higher amounts of cortical tau at 10 months compared to R955-hTau. However, in 20-months-old R962-hTau rats the levels of cortical tau decreased substantially to reach levels similar to age-matched wt rats. The decreased tau levels in 20-month-old R962-hTau rats are likely caused by the extensive brain degeneration and atrophy occurring at this age [31], as evidenced by the changes in brain structures and HT7 immunoreactivity (Fig. 2D) as well as by a decrease in the levels of neurofilament light chain (NfL) (Fig. 2E-F). Defects in the total amount of neurofilaments, the predominant structural component of the adult neuronal cytoskeleton [47, 48], would indicate a loss of neuronal integrity. Together with the line's characteristics illustrated in Fig. 1, this highlights that R962-hTau+/- rats display a stronger tau pathology phenotype than R955-hTau+/- rats and hence that tau pathology is stronger in 10-month-old R962-hTau+/- rats than in 20-month-old R955-hTau+/- rats.

Progressive tau and amyloid pathologies are accompanied by increased production of cytokines/chemokines

We next investigated whether the evolution of tau and amyloid pathologies coincided with significant changes in neuroinflammatory signals. In our rat models of tauopathy, an elevation in inflammatory molecules was mainly seen at late tau pathology stages. Thus, levels of IL-1β, TNF-α, and KC/GRO raised progressively with advancing pathology and were found significantly elevated in 20-month-old R962-hTau rats compared to age-matched wt rats. One exception was IFN-γ, which was elevated in 20-month-old R955-hTau rats but not in R962-hTau rats (Fig. 3A).

In contrast to the inflammatory profile in the tau pathology, in line with our previous publications [33, 49], we found that in McGill-APP rats, the cortical

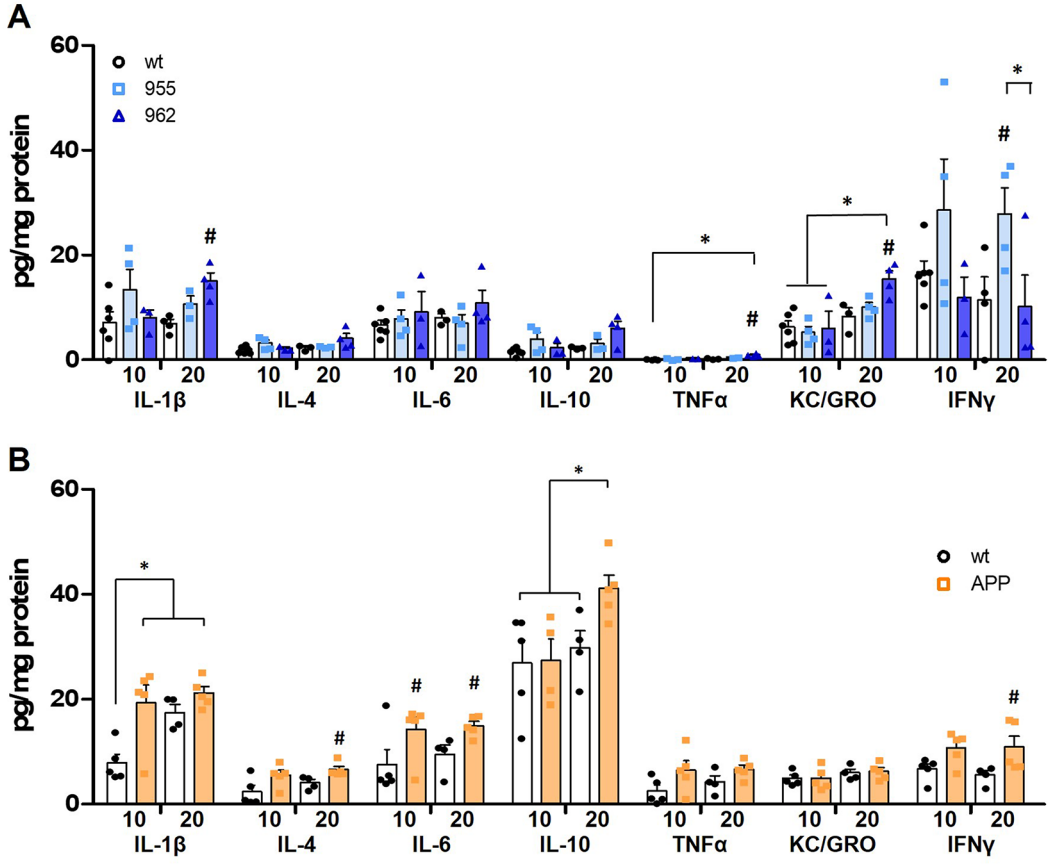

Fig. 3 Cortical production of cytokines and chemokines in progressive amyloid and tau pathologies. Cortical production of IL-1β, IL-4, IL-6, IL-10, TNFα, KC/GRO and IFNγ were measured by ECLIA in McGill-R-hTau rats (**A**) and in McGill-R-Thy1-APP rats (**B**). Values are expressed as means ± SEM ($n = 4–5$/group). Two-group comparisons were performed with the Mann-Whitney U test. Kruskal-Wallis with Dunn's post hoc tests was used for multiple comparisons. # $p < 0.05$ compared to age-matched wt rats. * $p < 0.05$ compared to other groups

production of the pro-inflammatory cytokines IL-1β and IL-6 was already significantly elevated (while TNF-α trended towards an elevation) compared to wt rats at pre-plaque stages and remained elevated at post-plaque stages. However, levels of the anti-inflammatory cytokines IL-4 and IL-10 and of IFN-γ were only found elevated at post-plaque stages (Fig. 3B).

Differential effect of amyloid and tau pathology on pro-inflammatory and pro-resolving lipid mediators

Given that the progressive amyloid and tau pathologies were accompanied by elevations in cytokines/chemokines, we then investigated the levels of pro-inflammatory and pro-resolving lipid mediators by LC-MS/MS. Our analyses revealed that in our models, the AA-derived prostaglandins D2 (PGD2), E2 (PGE2), and F2α (PGF2α) are more affected by tau pathology than by amyloid pathology (Fig. 4). Indeed, the levels of PGD2, PGE2, and PGF2α increased with the extent of tau pathology (Fig. 4B). R955-hTau+/- rats, which display modest levels of tau pathology, showed levels of prostaglandins similar to age-matched controls. In contrast, R962-hTau rats showed age- and pathology-dependent increases in the levels of these prostaglandins. By 20 months of age, representing late stages of tauopathy, the levels of these prostaglandins were considerably heightened and reached up to 7-fold higher levels compared to age-matched wt and R955-hTau rats. Interestingly, the levels of PGD2, PGE2, and PGF2α were negatively correlated with NfL (Fig. 4D) but did not correlate with Tau levels, suggesting that the levels of these lipid mediators are modulated in response to a secondary Tau-driven pathology rather than to the levels of Tau protein per se.

However, in response to amyloid pathology, the changes in AA-derived lipid mediators were more modest than in Tau transgenic rats (Fig. 4C). As such, post-plaque amyloid pathology coincided with a 2-fold increase in PGE2 levels in 16-month-old APP rats compared to age-matched wt rats while PGF2α trended towards an increase. Still, these levels are 10-fold lower than those detected in 20-month-old R962-hTau rats. Intriguingly, this rise seemed to be caused by an age-driven decrease in PGE2 and PGF2α levels in 16-month-old wt rats, given that the levels of PGE2 and PGF2α in 16-month-old McGill-APP rats are similar to 6-month-old wt and McGill-APP rats. Therefore, in McGill-APP transgenic rats, the presence of amyloid pathology counteracted the decline in prostaglandins due to aging.

Surprisingly, neither amyloid nor tau pathology affected the levels of the mono-hydroxy AA metabolites 5-HETE, 12-HETE and 15-HETE (hydroxyeicosatetraenoic acids), nor the levels of leukotriene B4 (LTB4) and lipoxin A4 (LXA4) (Supplemental Fig. 1). This suggests that, in our models, amyloid and tau pathologies have a greater impact on eicosanoids produced through the COX pathway than on those produced through the lipoxygenase (LO) pathway.

Likewise, our analyses revealed that the DHA-derived pro-resolving mediators resolvin D6 (RVD6) and 10,17 S-docosatriene (neuroprotectin D1, NPD1) are impacted differentially by tau and amyloid pathology in our models. However, the mono-hydroxy DHA metabolites 7-HDHA, 14 S-HDHA, 17 S-HDHA, and 20-HDHA were affected neither by amyloid nor tau pathology (Supplemental Fig. 2). Therefore, RVD6 isoforms RVD6_8.29, RVD6_8.46, and RVD6_8.56 show a stepwise decrease in their levels from the initial to the advanced stages of tauopathy (with significantly higher levels in 10-month-old R955-hTau rats compared to 20-month-old R962-hTau rats), but with a slower rate of decay than the effect of aging alone (Fig. 5B). As a result, in Tau transgenic rats, these RVD6 isoforms are positively correlated with NfL, representative of Tau-driven brain degeneration, but not with the levels of Tau (Fig. 5D). In addition, similar to RVD6_8.29, RVD6_8.46, and RVD6_8.56, NPD1 showed a stepwise decrease in its levels from the initial to the advanced stages of tauopathy, which is more pronounced than the effect of aging alone (Fig. 5B).

In comparison, pre-plaque amyloid pathology had a more pronounced effect on levels of DHA-derived mediators. In pre-plaque McGill-APP rats (6 months), levels of RVD6_8.29 and RVD6_8.46 isoforms were significantly heightened compared to age-matched wt rats. Levels of RVD6 isoforms decreased with amyloid pathology progression and by 16 months of age, levels of most RVD6 isoforms were similar to those seen in wt rats (Fig. 5C). Similarly, NPD1 was increased at pre-plaque stages of the evolving amyloid pathology but decreased at post-plaque stages to reach levels similar to age-matched wt rats.

The special case of RVD6_8.65 is worth mentioning. Levels of RVD6_8.65, the most abundant isoform, increased dramatically with age and the extent of tau pathology. Thus, RVD6_8.65 levels were significantly elevated in 20-month-old R955-hTau (4-fold) and R962-hTau rats (38-fold) compared to wt rats (Fig. 5B). Surprisingly, however, RVD6_8.65 did not correlate with NfL or Tau levels in transgenic rats (Fig. 5D). In contrast, RVD6_8.65 levels were higher in younger McGill-APP rats compared to age-matched wt rats (Fig. 5C).

As prostaglandin production depends on COX-2 levels and activity, we then examined whether COX-2 expression would be differentially expressed in cortical neurons in relation to tau pathology using immunofluorescence approaches and the AT8 antibody as well as an antibody recognizing COX-2. Contrary to our hypothesis, although COX-2 immunofluorescence levels trended towards an increase in relation to advancing tau pathology, this elevation did not reach statistical significance.

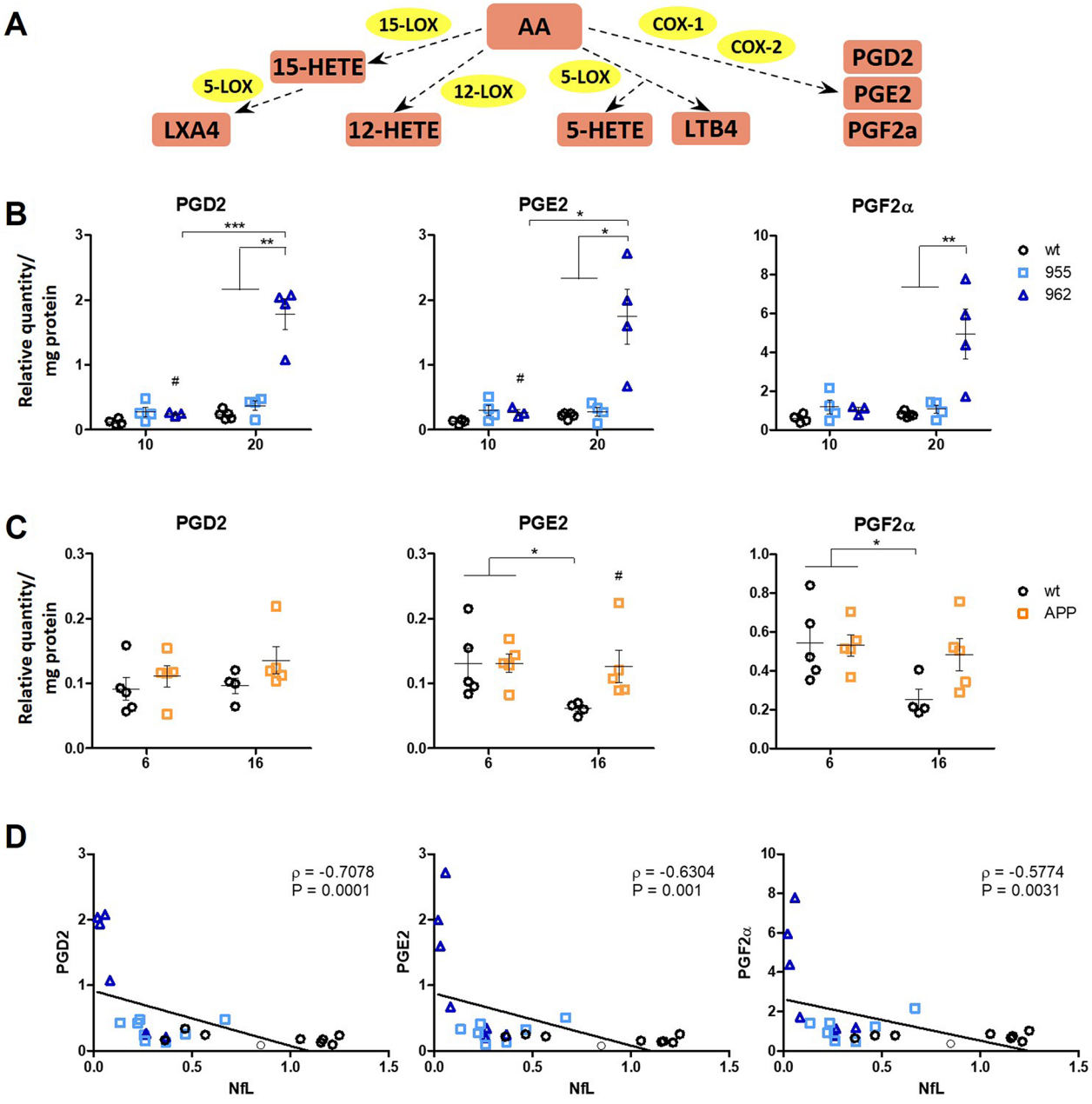

Fig. 4 Arachidonic acid-derived prostaglandins are highly increased at advanced stages of tau pathology. **A**. Arachidonic acid metabolism and production of eicosanoid lipid mediators including prostaglandins, leukotrienes and hydroxyeicosatetraenoic acids (HETEs). **B-C**. Levels of PGD2, PGE2, PGF2α in McGill-R-hTau rats (**B**) and in McGill-R-Thy1-APP rats (**C**). Two-group comparisons were performed with the Mann-Whitney U test. Kruskal-Wallis with Dunn's post hoc tests was used for multiple comparisons. # $p < 0.05$ compared to age-matched wt rats. * $p < 0.05$, ** $p < 0.01$,*** $p < 0.001$ compared to other groups. **D**. Levels of prostaglandins and NfL are inversely correlated as assessed by Spearman's correlation test

However, as for PGD2, PGE2 and PGF2α, COX-2 immunofluorescence levels were correlated with NfL but not with Tau5 immunoblotting signal intensity in transgenic rats (Supplemental Fig. 3). Additionally, within neurons, COX-2 and AT8 immunofluorescence intensities were weakly associated. This signifies that a cell burdened with pTau does not necessarily display higher COX-2 levels compared to other cells.

Given the differential effects of amyloid and tau pathologies on AA- and DHA-derived lipid mediators, we then examined their effect on the abundance of free very long-chain (>C24) polyunsaturated fatty acids (VLC-PUFAs) which are produced from long-chain PUFAs (LC-PUFAs; C20–C22; e.g., DHA, AA, and EPA) by the elongation of very-long-chain fatty acids-4 (ELOVL4) enzyme. Free FA24:6 and 26:6, the intermediate products

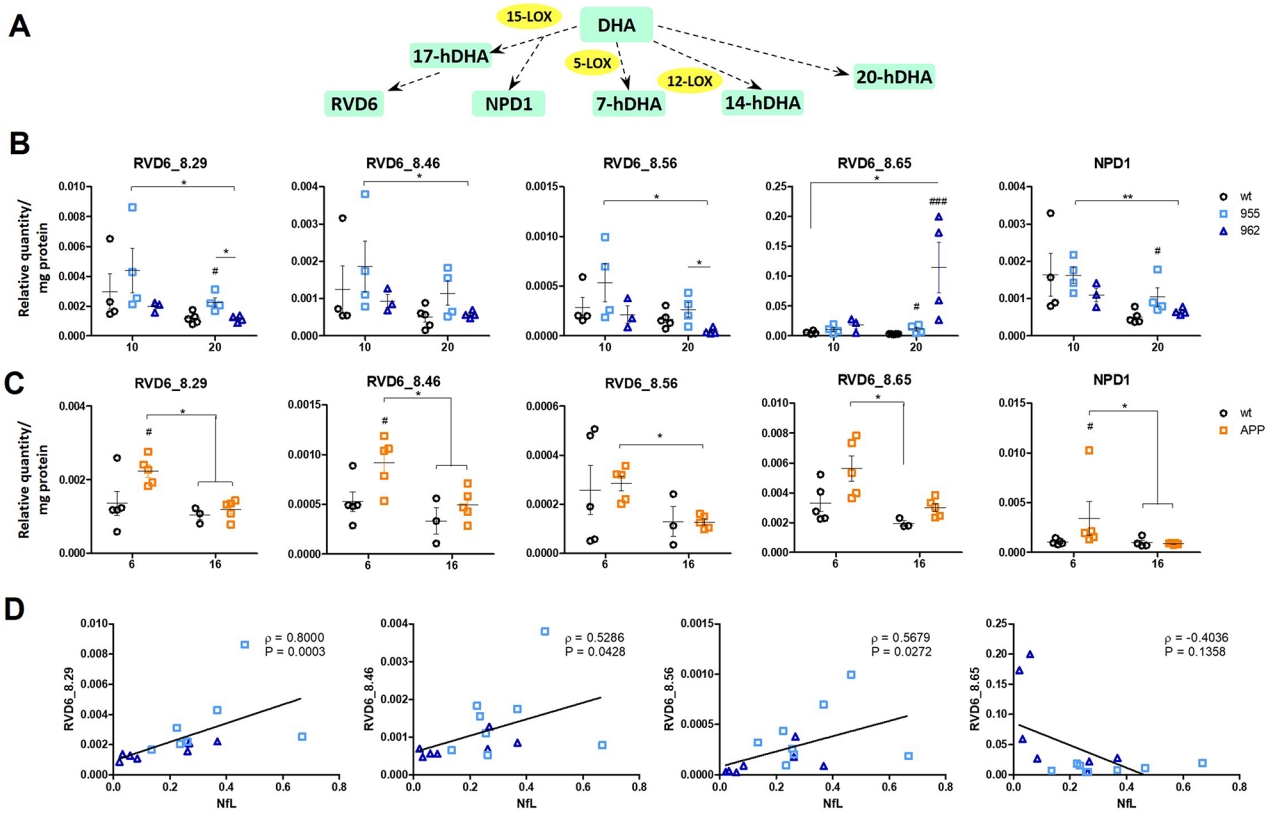

Fig. 5 Docosahexaenoic acid-derived bioactive lipid mediators are affected by amyloid and tau pathology. **A**. Docosahexaenoic acid metabolism and production of DHA-derived pro-resolving lipid mediators including Resolvin RVD6, protectin (NPD1) and polyunsaturated fatty acids. **B-C**. Levels of RVD6 isoforms and NPD1 in McGill-hTau rats (**B**) and in McGill-APP rats (**C**). Two-group comparisons were performed with the Mann-Whitney U test. Kruskal-Wallis with Dunn's post hoc tests was used for multiple comparisons. # $p < 0.05$, ### $p < 0.001$ compared to age-matched wt rats. * $p < 0.05$ compared to other groups. **D**. Levels of RVD6_8.29, RVD6_8.46, and RVD6_8.65 are directly correlated with NfL in McGill-hTau rats as assessed by a Spearman's correlation test

of the ELOVL4 pathway, and free FA32:6 n3 and FA34:6 n3, precursors of elovanoids, were elevated in 10-month-old R955-hTau rats when compared to their wt littermates, but not in 20-month-old R955-hTau rats nor in R962-hTau rats, suggesting that these VLC-PUFAs only respond at the very early stages of tau pathology (Fig. 6A). In contrast, amyloid pathology had no effect on the levels of these VLC-PUFAs (Fig. 6B).

Differential effect of amyloid and tau pathology on AA- and DHA-containing phospholipids

Since DHA and AA are implicated in physiological and pathological processes both as bioactive lipid mediators and as components of membrane phospholipids (PLs) [50–52], the later affecting membrane-based cellular processes [53, 54], we then examined the impact of the amyloid and tau pathologies on the abundance of DHA- and AA-containing PLs (Fig. 7).

We found alterations in the fatty acyl chain composition of PLs in both tau and amyloid transgenic rat models. As expected, these alterations coincided better with the extent of pathology than with aging alone. Thus, few changes in PLs abundance were seen in 10-month-old R955-hTau rats. Interestingly, in 20-month-old R955-hTau heterozygous rats a moderate level of tau pathology, as represented by an elevation in pTau (Ser202, Thr205; AT8), but in the absence of modifications at other tau epitopes and neuronal loss, as previously reported [29] and summarized in Fig. 1, caused alterations in 15 PLs, including a significant increase of DHA-containing PLs and, to a lesser extent, a decrease in AA-containing PLs compared to age-matched wt littermates (Supplemental Tables 1 and Fig. 7A). The PLs affected were mainly phosphatidylcholines (PC) and phosphatidylethanolamines (PE). In 10-month-old R962-hTau rats displaying increased tau phosphorylation, conformational changes, and aggregation in the absence of neuronal loss, there were alterations in 11 PLs equally distributed between DHA- and AA-containing species, mostly PCs and PEs. However, the direction of the changes in PLs contrasted with that observed in 20-month-old R955-hTau rats. There was an increase in AA-containing species and a decrease in DHA-containing species. This increase in AA-containing species further progressed in advanced

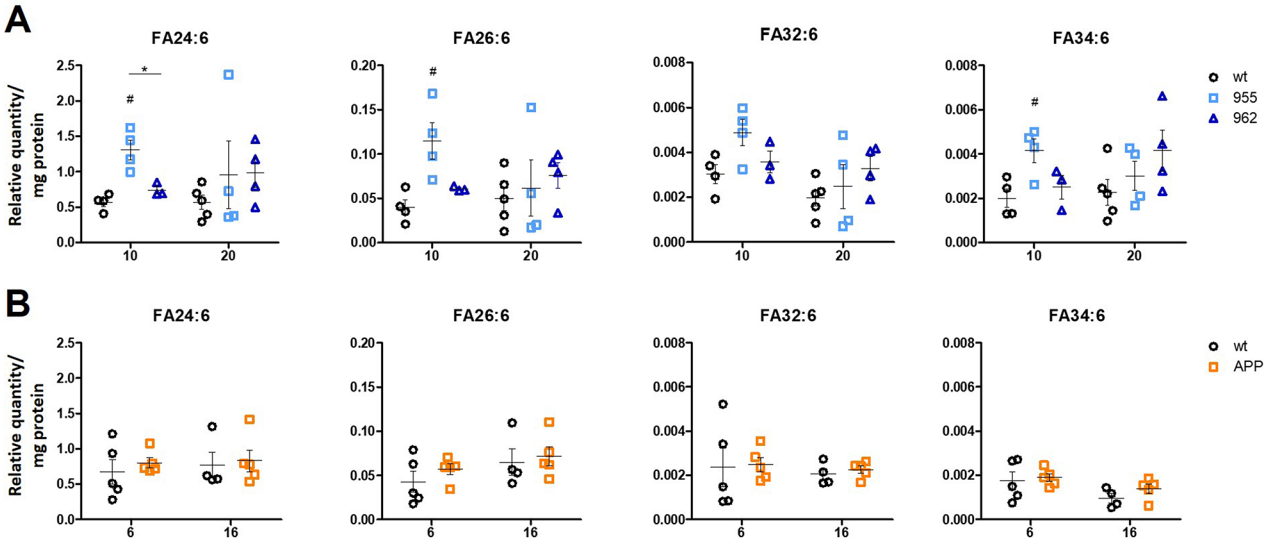

Fig. 6 Abundance of free very long-chain (> C24) polyunsaturated fatty acids (VLC-PUFA) is heightened in early-stage tau pathology. **A.** Levels of FA24:6, FA26:6, FA32:6, FA34:6 are increased in 10-month-old McGill-R955-hTau rats but not at an older age nor in McGill-R962-hTau rats. Levels of these PUFAs are not affected by amyloid pathology (**B**). Two-group comparisons were performed with the Mann-Whitney U test. Kruskal-Wallis with Dunn's post hoc tests was used for multiple comparisons. # $p < 0.05$ compared to age-matched wt rats. * $p < 0.05$ compared to other groups

tau pathology. As expected, the brain of 20-month-old R962-hTau rats, which display extensive tau pathology, neurodegeneration, and brain atrophy, showed the highest number of changes in PLs abundance. Notably, there was an elevation predominantly in AA-containing PLs but also in some DHA-containing PLs distributed equally between PCs, PEs, phosphatidylserines (PS), and sphingomyelins (SM).

Accordingly, at the individual level, in response to progressing tau pathology, most DHA-containing PLs showed a stepwise decrease in their levels that was independent of aging (Fig. 7A-B). Consequently, 20-month-old R955-hTau rats displayed significantly higher levels of those DHA-containing PLs than age-matched wt and 20-month-old R962-hTau rats. Conversely, some DHA-containing PLs showed a stepwise increase in their levels (PC34:7, PC42:10, PE40:8, PS48:10). In contrast, the increase in AA-containing PLs occurred mostly at stages with significant tau pathology in 10- and 20-month-old R962-hTau rats. Remarkably, while most PLs were elevated only at 20 months of age, some PLs were elevated at 10 months to stabilize (PC38:4, PC40:4, PE38:4, PE40:4) or even decrease (PS44:5) afterward (Fig. 7A-B).

The pattern of alterations in PLs levels in response to amyloid pathology in McGill-APP transgenic rats was different from that of tau transgenic rats (Supplemental Tables 1 and Fig. 7A). At early pre-plaque stages (6 months), only 5 PLs were impacted: most of them were AA-containing PLs and showed increased levels. At post-plaque stages (16 months), McGill-APP rats showed a marked decrease in DHA-containing PLs and an increase in AA-containing PLs, which was modest in comparison to the rise seen in response to late tau pathology.

Discussion

In the present study, we explored the effect of an evolving amyloid and tau pathology, separately, on the phospholipid composition of cell membranes as well as on bioactive lipid mediators of inflammation synthesized from phospholipids through the action of phospholipase A. This study provides a much-needed landscape of the changes in lipid mediators provoked by tau pathology as represented in transgenic rat models recapitulating the staging of human-like tauopathy [30, 31]. Furthermore, our findings show that tau pathology has a more pronounced effect on the levels of phospholipids and bioactive lipid mediators than amyloid pathology. These aspects are of significance given that tau pathology is ultimately the main cause of AD dementia. Cerebral amyloid deposition in AD pathology is poorly associated with the severity of cognitive symptoms [55–57]. In contrast, tau pathology emerges much closer to cognitive symptomatology [58–65], and it is associated with grey matter loss [66]. The close relationship between tauopathy and cognition is also present in the healthy aging brain [67, 68].

As summarized in Fig. 8, we found that in tau transgenic rats, the initial tau pathology preceding increased tau phosphorylation at Ser202-Thr205 (AT8 immunoreactivity) [29], as represented in 10-month-old R955-hTau +/- rats, is accompanied by elevations in intermediates of VLC-PUFA synthesis and in IFN-γ. As these elevations are specific to this early pathology stage and return

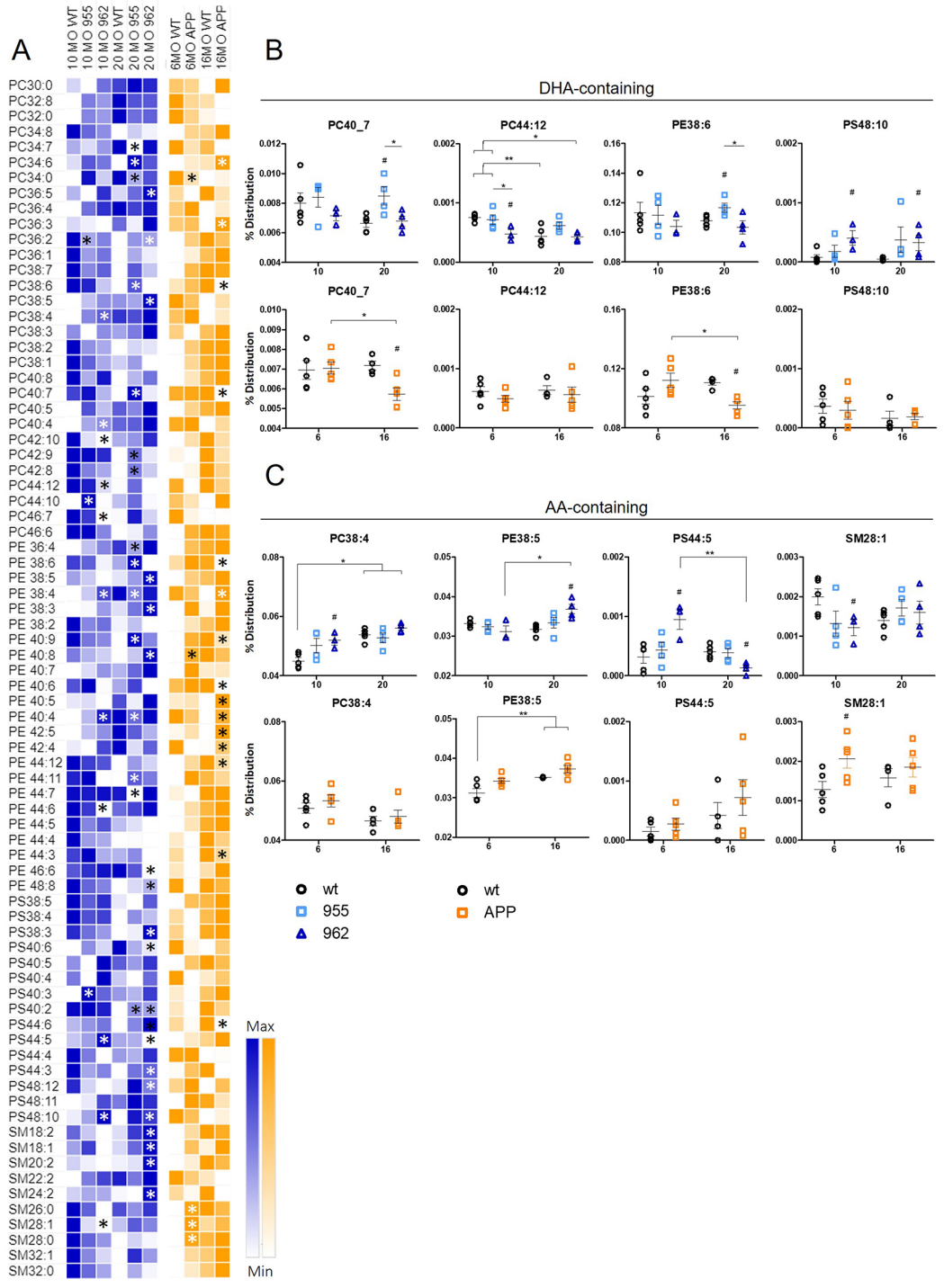

Fig. 7 Altered abundance of DHA- and AA-containing phospholipids in response to amyloid and tau pathology. **A**. Heat map analysis of PCs, PEs, PSs, and SMs of 10- and 20-month-old McGill-R955-hTau, McGill-R962-hTau and age-matched wt rats (left) and of 6- and 16-month-old McGill-R-Thy1-APP and age-matched wt rats (right). Rows represent mean values of phospholipids and columns represent different ages and genotypes as indicated. **B-C**. Scatter plots of selected DHA- and AA-containing phospholipids show a decrease in DHA-containing phospholipids and an increase in AA-containing phospholipids in both APP and hTau rats. Two-group comparisons were performed with the Mann-Whitney U test. Kruskal-Wallis with Dunn's post hoc tests was used for multiple comparisons. # $p < 0.05$, ### $p < 0.001$ compared to age-matched wt rats. * $p < 0.05$, ** $p < 0.01$ compared to other groups

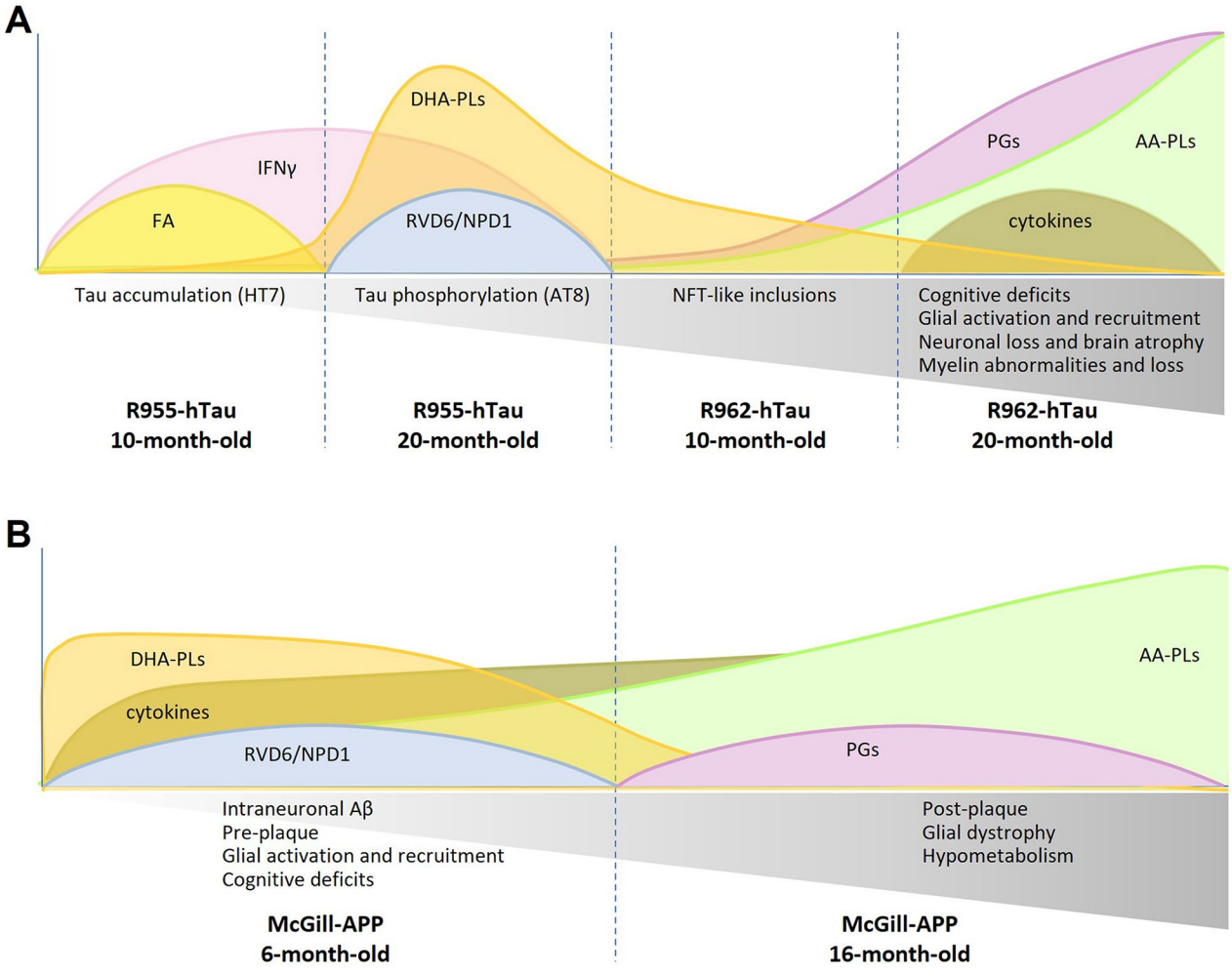

Fig. 8 Summary of the changes observed in this study. **A**. Changes in R955-hTau and R962-hTau rats. **B.** Changes in McGill-APP rats

to baseline levels after tau aggregation, we may speculate that a sudden rise in their levels would help predict a forthcoming increment in tau pathology in combination with classical markers of tau pathology. This aspect calls for further investigations. Similarly, we found that an elevation in pTau Ser202-Thr205 (AT8 immunoreactivity), prior to tau misfolding and aggregation, as represented in 20-month-old R955-hTau +/- rats, is accompanied by elevations in DHA-containing PLs, IFN-γ, RVD6, and NPD1 as well as a decrease in AA-containing PLs. These changes are also specific to this stage and wane after tau aggregation. Furthermore, the establishment of NFT-like inclusions prior to neuronal death and cognitive decline, as revealed in 10-month-old R962-hTau +/- rats, is accompanied by a modest reduction in DHA content and moderate elevations in AA-containing PLs as well as in PGD2, PGE2, and PGF2α. Finally, the presence of a full-blown tauopathy, as displayed in 20-month-old R962-hTau +/- rats, is characterized by signification elevations in cytokines, prostaglandins, and AA-containing PLs.

In contrast, in McGill-APP transgenic rats, the accumulation of iAβ before the deposition of plaques (6-month-old) is accompanied by elevations in cytokine expression, RVD6 and NPD1 levels, and AA-containing PLs (PE and SM). After plaque deposition (16-month-old), cytokine levels remain elevated while there is a drop in RVD6, NPD1, and DHA-containing PLs. In addition, there is an increase in AA-containing PLs (PC and PE) as well as a stabilization in PGD2, PGE2, and PGF2α levels, which do not decrease with aging as they do in wt rats.

A striking difference between the two pathologies is the timing of production of cytokines in amyloid and tau pathology, which represents an early and late pathological feature, respectively. Therefore, elevations in IL-1β, TNFα, and KC/GRO could only be detected at advanced stages of tau pathology, as recapitulated in 20-month-old R962-hTau transgenic rats. It is worth noting that this cohort is the only one displaying overt glial activation. Only minor changes in microglia morphology are observed in 10-month-old R962-hTau, while

glial changes are absent in R955-hTau rats at both time-points. Therefore, the production of those cytokines seems to be associated with glial activation. Elevations in these cytokines have been reported in post-mortem brain tissue from individuals with AD and other tauopathies, including frontotemporal dementia and parkinsonism linked to chromosome 17 (FTDP-17) and in mouse models carrying tau mutations [69–72]. In contrast, IFN-γ was only elevated in early tau pathology, as represented in 20-month-old R955-hTau transgenic rats, prior to tau's conformational changes and aggregation, glial activation and overt cognitive deficits [30]. This observation is in line with studies showing that high IFN-γ levels are only detected in mild, but not in severe, stages of AD [73].

On the other hand, an increased cytokine production (IL-1β, IL-6,) was detected from early pre-plaque stages of the amyloid pathology (6-month-old McGill-APP rats) and remained elevated at post-plaque stages while other cytokines (most of them displaying anti-inflammatory properties) came about at later stages (IL-4, IL-10, IFNγ). This scenario would agree with our previous reports of a pro-inflammatory process occurring at pre-plaque stages of amyloid pathology including elevations in COX-2, IL-1β, TNFα, IL-6, CCL-2, CCL-3 and CX3CL1 [33, 49, 74, 75]. This inflammatory process is initiated in Aβ-burdened hippocampal neurons and coincides with microglia activation and recruitment towards those neurons [33, 49, 74, 75]. These findings reinforce the notion that neurons are the first inflammatory agents in response to amyloid but not to tau pathology, and they highlight differences in the neurochemical pathways activated in response to the two central AD pathologies.

Alternatively, and importantly, this may also suggest that oligomerization of amyloid and tau is a prerequisite for the initiation of inflammatory responses. Indeed, oligomeric Aβ, as revealed by neuronal NU-1 immunoreactivity [76], could already be detected inside neurons of the subiculum, CA1, CA3, and cortical layer V in 5-month-old McGill-APP rats presenting intraneuronal production of cytokines [33]. On the other hand, in R955-hTau heterozygous rats, the occurrence of tau oligomerization as detected using the tau oligomer-specific antibody T22 was only revealed at 24–26 months of age (months after the last time-point examined in this study) and coincided with neuronal loss [30]. Although not demonstrated here, one can safely speculate that oligomeric tau species are present in 20-month-old R962-hTau heterozygous rats displaying advanced tau pathology and neuronal loss.

This dichotomy in inflammatory responses to amyloid vs. tau pathologies was reflected in the production of lipid mediators derived from AA and DHA. Our findings showed that while amyloid pathology had a modest effect on the production of AA-derived pro-inflammatory prostaglandins [77], the advanced tau pathology, as reflected in heterozygous R962-hTau rats, induced significant increases in PGD2, PGE2, and PGF2α. Despite these differences, in both pathologies, increased prostaglandin production was a late pathological event, occurring after the aggregation of Aβ and tau into neuritic plaques or NFT-like inclusions.

In addition to their role in neuroinflammation [78–80], prostaglandins, in particular PGD2 and PGE2, play key roles at the synapse and the neurovascular unit where they regulate synaptic transmission and cerebral blood flow. PGE2 has also been shown to mediate the effects of IL-1β on learning impairments in rats [81, 82], to suppress myeloid cell bioenergetics in aging mice [83] and to regulate neuronal apoptosis and necrosis [84–87]. Importantly, in the context of an inflammatory response, PGE2 induces lipid mediator class-switching by inhibiting 5-LOX translocation from the cytoplasm to the nucleus, thereby abrogating leukotriene synthesis and favoring lipoxin synthesis, which stimulates inflammation resolution [88].

The relationship between prostaglandins and amyloid pathology in AD has been extensively studied [89–97]. PGE synthase has been found increased in AD brains, and PGD synthase was found in amyloid plaques in AD brains and Tg2576 mice [98, 99]. Additionally, deletion of the PGE2 EP3 receptor reduced pro-inflammatory cytokine production, oxidative stress, and production of Aβ peptides in mouse models of amyloid pathology [94, 100, 101]. Considering the above, the small effect of amyloid pathology on prostaglandin levels in McGill-APP rats was somewhat surprising. However, our findings do recapitulate those from APP NL-G-F Knock-in mice where PGD2, PGE2, and PGF2α were only found elevated in 18-month-old mice, i.e., more than 15 months after the initiation of plaque deposition [102]. Similarly, they align with findings reported in J20 mice where in cortical tissue, only minor elevations in LTB4 were observed, while AA, AA-derived metabolites, and COX metabolites remained unchanged. However, significant alterations in AA, AA-derived metabolites, and metabolites of LOX, COX, and CYP were found in hippocampal homogenates [103, 104].

In comparison, information on the interaction of prostaglandins and tau is scarce. PGF2α was reported to mediate the effects of TNF-α and Zn2+in stimulating tau phosphorylation [105]. It was also demonstrated in vitro that PGJ2 induces caspase-mediated cleavage of tau, generating the aggregation-prone Δtau [106]. In addition, pharmacological blockade of COX-1/2 and 5-LOX with flavocoxid blunted both Aβ and tau pathology in 3xTg-AD mice [107], suggesting that prostaglandins play a role in both pathologies.

Therefore, in addition to revealing a relationship between tau pathology and prostaglandins, the present findings would suggest that tau misfolding and aggregation are required to induce a burst of PGD2, PGE2, and PGF2α production coinciding with microglia phenotypic changes [31]. The production of prostaglandins is further amplified at late tau pathology stages, presenting overt microglia activation, cytokine production, and neuronal cell death where it correlates with NfL levels rather than simply tau levels. This novel observation is of potential significance for our understanding of the pathology, especially as it does not extend to LOX metabolites. Our findings may also suggest that in AD, the increases in prostaglandins are mostly driven by tau pathology, although a contribution of late-stage Aβ plaque pathology cannot be ruled out.

However, the mechanisms underlying such prostaglandin elevation remain obscure. One possible explanation could be the stimulation of COX-2 levels and activity by tau pathology. COX-2 plays a central role in prostaglandin production and acts as a neuronal modulator [108]. It has been shown that in P301S mice, tau-immunoreactive nerve cells in the brainstem and spinal cord were strongly immunoreactive for IL-1β and COX-2 [109]. It has also been shown that in the brains of AD patients and individuals with Down syndrome with AD pathology, COX-2 induction notably occurs in neurons bearing NFTs and in damaged axons [110]. However, using immunofluorescence approaches we could not demonstrate unequivocally that COX-2 levels are affected by tau pathology rather than by aging alone and AT8-immunoreactive neurons do not display increased COX-2 levels compared to other cortical cells. In addition, COX-2 levels, as prostaglandins, do not correlate with tau levels as measured by western blotting (Tau5 immunoreactivity) but rather with NfL diminution. This observation aligns with the work of Oka and collaborators showing increased COX-2 levels in damaged axons of AD and DS individuals [110]. Axons are likely damaged in our hTau rats given the decreased NfL levels coinciding with tau pathology [110].

COX-2 is also known to be induced by inflammatory stimuli, including pro-inflammatory cytokines such as IL-1β, mediated through protein kinase C and mitogen-activated protein kinases [111, 112]. Interestingly, IL-1β levels are elevated at late pathology stages in R962-hTau rats. However, previous research from our group has shown that elevated IL-1β and COX-2 levels are also present in McGill-APP rats [49], which do not exhibit increased prostaglandin levels. This suggests that the increase in PGD2, PGE2 and PGF2α in the brain of rats reproducing advanced tau pathology potentially involves also other mechanisms yet to be identified .The elevated levels of PGD2, PGE2, and PGF2α observed in the brains of rats exhibiting advanced tau pathology could also potentially be linked to increased COX-2 enzymatic activity facilitated by tau-induced extrasynaptic NMDAR activation rather than its levels. Tau pathology has been shown to promote extrasynaptic NMDAR activation, which is associated with neurodegeneration [113]. This form of NMDAR activation has also been found to notably elevate COX-2 enzymatic activity by increasing AA release. In contrast, synaptic NMDAR activation primarily induces COX-2 expression with relatively lower prostaglandin (PG) production [114].

These investigations also revealed a contrasting effect of amyloid and tau on the production of DHA-derived pro-resolving lipid mediators. As such, RVD6 and NPD1 were significantly elevated in pre-plaque amyloid pathology. However, RVD6 and NPD1 were little affected by the evolving tau pathology and were only increased in 20-month-old R955-hTau +/- rats, which display an elevation in pTau Ser202-Thr205 (AT8 immunoreactivity) [29]. Despite these differences, in both pathologies, RVD6 and NPD1 elevations seemed limited to early disease stages prior to amyloid and tau misfolding and aggregation. The cause and significance of these transient elevations in RVD6 and NPD1 remain unknown. The notion that they might represent an attempt at counteracting the deleterious actions of the initial disease-aggravating cytokine production in pre-plaque McGill-APP rats could be advanced [33, 49, 74, 75]. However, their marginal elevation in 20-month-old R955-hTau +/- rats remains unresolved, as the only evidence of an ongoing inflammatory process is the increased IFN-γ levels.

In addition to their effects on inflammation, pro-resolving lipid mediators improve neuronal survival and increase Aβ phagocytosis [25, 115–118]. Decreased levels of RvD1, LXA4, and NPD1 have been reported in the brain and CSF of AD patients and in AD models [24, 25, 27, 116, 117]. Administration of RVE1 and LXA4 in AD models reduced Aβ plaque deposition, reversed the inflammatory process, and ameliorated cognition [119]. NPD1, which is also triggered by oxidative stress and activation of neurotrophins [120], was shown to enhance neuron survival and alleviate amyloidogenic processing of APP [27, 115, 121–123]. There are no reports on RVD6 levels and function in AD. However, RVD6 was reported as decreasing inflammation and increasing nerve regeneration in the damaged cornea [124].

Moreover, this study provided evidence that the early tau pathology (prior to tau phosphorylation at Ser202, Thr205 (AT8 immunoreactivity)) as represented in 10-month-old R955-hTau rats [29], could be signaled by a sudden and transient increase in free FA24:6 and 26:6, the intermediate products of the ELOVL4 pathway, and free FA32:6 n3 and FA34:6 n3, which are precursors of elovanoids [125–129]. Such elevation was not present in rats with more pronounced tau pathology or

in McGill-APP rats. This may be suggestive of an initial reparative effect of VCL-PUFAS against tau pathology. However, the mechanisms and function underlying this elevation remain to be determined.

VLC-PUFAs are highly enriched in the brain and modulate neuronal function and health [130, 131], including the release of neurotransmitters [132, 133]. Oxidative stress and oligomeric Aβ peptides are known to trigger the release of VLC-PUFAs. Changes in the levels of VLC-PUFAs can modify the structure, fluidity, and function of cellular membranes [134–139] and lead to cellular dysfunction and death [132, 133, 140, 141]. Still, there is very limited information regarding alterations in VLC-PUFAs contained in phospholipid molecular species in the brain affected by AD and other tauopathies. Accumulation of VLC-PUFAs due to peroxisomal dysfunction [142] was reported in the cortex of AD cases with Braak stage V-VI pathology [143], and their levels correlated with cognitive deficits. In contrast, a deficiency of VLC-PUFAs in PCs was reported in the retina of 5xFAD mice displaying an accelerated amyloid pathology [144].

As VLC-PUFAs are found mainly in the phospholipids PC, PE, PS, and SM, we examined levels of phospholipids as precursors to produce bioactive lipid mediators. Once again, tau pathology induced more pronounced changes in the distribution of phospholipids than amyloid. The progressive tau pathology first induced an increase in DHA-containing PLs coinciding with p-Tau at pSer202-pThr205 (AT8 immunoreactivity), which was followed by a shift towards increased AA-containing PLs when tau conformational changes and NFT-like inclusions developed. This suggests the existence of a tilting point in the balance between DHA and AA-containing PLs, which would depend on tau oligomerization and conformational changes. It may also suggest that AA-containing PLs are more toxic to cells.

In contrast, progressing amyloid pathology was dominated by an elevation in AA-containing PLs, which were accompanied by decreases in DHA-containing PLs at post-plaque stages. The present findings would align with those reported in APP NL-G-F Knock-in mice, showing a marked increase in AA-containing PLs and a decrease in DHA-containing PLs at late amyloid pathology stages [102]. They also corroborate the described elevations in 3 AA-containing PLs in cortical tissue from FTD cases, which were strongly correlated with ELOVL4 levels and increased with disease severity and neurodegeneration [145]. Decreased brain phospholipid levels and alterations in brain phospholipid metabolism have also been noted in both the white and grey matter [146–149] of the AD brain. These alterations evolve with AD progression and would play different roles in the white and gray matter. Changes in the grey matter are minor compared to those in the white matter but are associated with vulnerability to oxidative stress while the changes in the white matter would be associated with a protective profile [149]. In the present study, there was no evident loss of phospholipids in cortical tissue. Rather, there was an alteration in phospholipid species with a drastic accumulation of AA-containing PLs in 20-month-old R962-hTau rats, which coincided with myelin loss and overall brain atrophy [31].

The initial rise in DHA-containing PLs, as well as the more dramatic changes at advanced tauopathy stages, suggest that amyloid and tau have a different effect on the content in PLs and, therefore, on the properties, structure, and function of cellular membranes. These alterations may explain, at least partially, the differences found here in lipid mediators. How amyloid and tau specifically affect the content in PLs of cellular membranes remains unknown. Tau interacts with different components of cellular membranes, including lipids, proteoglycans, and membrane proteins, as eloquently reviewed by Bok and colleagues 2021 [150]. This interaction modulates the aggregation and toxic properties of tau. Of interest to this study, two hexapeptide motifs of the microtubule-binding-domain of tau are critical for the formation of the tau-phospholipid complexes, which promote folding and fibril formation in acidic pH and are toxic to primary hippocampal neurons [151–154]. Likewise, Aβ binds directly to membrane lipids and modifies the lipid bilayer structure [155–157].

Conclusions

This study provides a landscape of changes in lipid mediators in the evolving amyloid and tau pathologies, separately. Our findings reveal that tau has a more pronounced effect on lipid mediators than amyloid pathology, especially regarding prostaglandins, VLC-PUFAs and phospholipids. Still, both pathologies display similar features in the timing of the production of lipid mediators. Therefore, both pathologies showed increased production of pro-resolving lipid mediators NPD1 and RVD6 at pathology stages preceding Aβ and tau misfolding and aggregation. They also illustrate an increased PGD2, PGE2, and PGF2α production as well as elevated AA-containing PLs and reduced DHA-containing PLs at late pathological stages when Aβ and tau misfolding and aggregation are established. These findings reveal a complex balance between pro-inflammatory and pro-resolving processes, which, in combination with classical AD markers, may help identify disease stages as well as differentiate AD from other tauopathies at stages preceding overt neuronal loss and, therefore, stages more prone to intervention.

Limitations and considerations

This study is exploratory in nature, distinguished by its utilization of LC-MS/MS to examine the pro-inflammatory and pro-resolving lipidome in samples from two distinct transgenic models of AD-like pathology. However, additional research involving larger cohorts for each group is warranted, particularly to expand the number of age-matched animals. This is especially important given the varied profile of changes observed with aging and model.

Additional limitations of this study include the lack of distinction between the sexes of the animals for each cohort in the sample analysis. This could influence experimental outcomes, hinder the complete understanding of certain physiological events, contribute to biased interpretations, and limit the generalizability of findings.

Abbreviations

AA	Arachidonic acid
AD	Alzheimer's disease
APP	Amyloid precursor protein
Aβ	Amyloid beta
CAMKIIα	Calcium/calmodulin-dependent protein kinase type II subunit alpha
COX	Cyclooxygenase
CSF	Cerebrospinal fluid
CYP	Cytochrome P450
DHA	Docosahexaenoic acid
ELOVL4	Elongation of very-long-chain fatty acids-4
EPA	Eicosapentaenoic acid
FTDP	17-Frontotemporal dementia and parkinsonism linked to chromosome 17
GFAP	Glial fibrillary acidic protein
HDHA	Hydroxy docosahexaenoic acid
HETE	Hydroxyeicosatetraenoic acid
HRP	Horseradish peroxidase
IFN	γ-Interferon gamma
IL	Interleukin
KC/GRO	Keratinocyte chemoattractant (KC)/human growth-regulated oncogene (GRO)
LA	Linoleic acid
LC	MS/MS-Liquid Chromatography with tandem mass spectrometry
LOX	Lipoxygenase
LTB4	Leukotriene B4
LXA4	Lipoxin A4
MAPT	Microtubule associated protein tau
MCI	Mild cognitive impairment
NFT	Neurofibrillary tangle
NGS	Normal goat serum
NPD1	Neuroprotectin D1; 10,17 S-docosatriene
NSAIDs	Nonsteroidal anti-inflammatory drugs
PBS	Phosphate buffered saline
PC	Phosphatidylcholines
PE	Phosphatidylethanolamines
PGD2	Prostaglandin D2
PGE2	Prostaglandin E2
PGF2α	Prostaglandin F2α
PLA2	Phospholipase A2
PLs	Phospholipids
PS	Phosphatidylserines
PUFAs	Polyunsaturated fatty acids
RVD6	Resolvin D6
SCI	Subjective cognitive impairment
SM	Sphingomyelins
TNF	α-Tumour necrosis factor alpha
VLC	PUFAs-Very long chain polyunsaturated fatty acids
Wt	Wild type

Supplementary Information

The online version contains supplementary material available at https://doi.org/10.1186/s12974-024-03184-7.

Supplementary Material 1

Supplementary Material 2

Supplementary Material 3

Supplementary Material 4

Supplementary Material 5

Supplementary Material 6

Acknowledgements

We thank and acknowledge Dr. Alfredo Ribeiro-da-Silva for training, technical assistance and access to the Axioplan 2 imaging microscope. We are grateful to Dr. Jörg Hermann Fritz and Ms. Nailya Ismailova for access and technical assistance with the MesoScale Discovery SECTOR Imager 6000 and software.

Author contributions

SDC, NGB, and ACC conceptualized and designed the study and edited the final manuscript. SDC, JTE, and JCM collected brain tissue samples and performed IHC procedures. SDC carried out ECLIA analyses. CS and SDC performed Western blot analyses. QB performed IF procedures and analyses. NGB, M-AIK, SB, and BJ prepared samples, performed LC-MS/MS lipidomics, and analyzed data. SDC performed data analyses and wrote the manuscript.

Funding

This study was supported by the Canadian Institute of Health Research (CIHR-PJT-186111), the Healthy Brains Healthy Lives and BrainsCAN McGill - Western Collaboration Grant (MWCG), the Morris and Rosalind Goodman Family Foundation and the Sylvester and Pauline Chuang Foundation to ACC's Laboratory. This study was also supported by the EENT Foundation of New Orleans (NGB). ACC is the holder of the Charles E. Frosst/Merck-endowed Chair in Pharmacology and a member of the Canadian Consortium on Neurodegeneration in Aging. SDC is the holder of the Charles E. Frosst/Merck Research Associate position.

Data availability

No datasets were generated or analysed during the current study.

Declarations

Ethics approval and consent to participate

All animal work was carried out under strict adherence to the guidelines set down by the Canadian Council of Animal Care and was approved by the Animal Care Committee of McGill University.

Consent for publication

Not applicable.

Competing interests

The authors declare no competing interests.

Author details

[1]Department of Pharmacology & Therapeutics, McGill University, 3655 Promenade Sir William Osler, Room 1210, Montreal H3G 1Y6, Canada
[2]Neuroscience Center of Excellence, School of Medicine, Louisiana State University Health New Orleans, 2020 Gravier Street, Suite D, New Orleans, LA 70112, USA
[3]Department of Cell Anatomy and Cell Biology, McGill University, Montreal H3A 0C7, Canada
[4]Department of Neurology and Neurosurgery, McGill University, Montreal H3G 1Y6, Canada
[5]Department of Pharmacology, Oxford University, Oxford OX1 3QT, UK

Received: 19 April 2024 / Accepted: 23 July 2024
Published online: 30 July 2024

References

1. Jack CR Jr., Knopman DS, Jagust WJ, Shaw LM, Aisen PS, Weiner MW, et al. Hypothetical model of dynamic biomarkers of the Alzheimer's pathological cascade. Lancet Neurol. 2010;9:119–28.
2. Harold D, Abraham R, Hollingworth P, Sims R, Gerrish A, Hamshere ML, et al. Genome-wide association study identifies variants at CLU and PICALM associated with Alzheimer's disease. Nat Genet. 2009;41:1088–93.
3. Lambert JC, Heath S, Even G, Campion D, Sleegers K, Hiltunen M, et al. Genome-wide association study identifies variants at CLU and CR1 associated with Alzheimer's disease. Nat Genet. 2009;41:1094–9.
4. Holloway OG, Canty AJ, King AE, Ziebell JM. Rod microglia and their role in neurological diseases. Semin Cell Dev Biol. 2019;94:96–103.
5. Brouwers N, Van Cauwenberghe C, Engelborghs S, Lambert JC, Bettens K, Le Bastard N, et al. Alzheimer risk associated with a copy number variation in the complement receptor 1 increasing C3b/C4b binding sites. Mol Psychiatry. 2012;17:223–33.
6. Lambert JC, Ibrahim-Verbaas CA, Harold D, Naj AC, Sims R, Bellenguez C, et al. Meta-analysis of 74,046 individuals identifies 11 new susceptibility loci for Alzheimer's disease. Nat Genet. 2013;45:1452–8.
7. Jonsson T, Stefansson H, Steinberg S, Jonsdottir I, Jonsson PV, Snaedal J, et al. Variant of TREM2 associated with the risk of Alzheimer's disease. N Engl J Med. 2013;368:107–16.
8. Akiyama H, Barger S, Barnum S, Bradt B, Bauer J, Cole GM, et al. Inflammation and Alzheimer's disease. Neurobiol Aging. 2000;21:383–421.
9. Frost GR, Jonas LA, Li YM, Friend. Foe or both? Immune Activity in Alzheimer's Disease. Front Aging Neurosci. 2019;11:337.
10. Wilcock DM. Neuroinflammatory phenotypes and their roles in Alzheimer's disease. Neurodegener Dis. 2014;13:183–5.
11. Cuello AC. Early and late CNS inflammation in Alzheimer's Disease: two extremes of a Continuum? Trends Pharmacol Sci. 2017;38:956–66.
12. Franceschi C, Bonafe M, Valensin S, Olivieri F, De Luca M, Ottaviani E, et al. Inflamm-aging. An evolutionary perspective on immunosenescence. Ann N Y Acad Sci. 2000;908:244–54.
13. Franceschi C, Capri M, Monti D, Giunta S, Olivieri F, Sevini F, et al. Inflammaging and anti-inflammaging: a systemic perspective on aging and longevity emerged from studies in humans. Mech Ageing Dev. 2007;128:92–105.
14. McGeer PL, Rogers J. Anti-inflammatory agents as a therapeutic approach to Alzheimer's disease. Neurology. 1992;42:447–9.
15. Jaturapatporn D, Isaac MG, McCleery J, Tabet N. Aspirin, steroidal and non-steroidal anti-inflammatory drugs for the treatment of Alzheimer's disease. Cochrane Database Syst Rev. 2012:CD006378.
16. Meyer PF, Tremblay-Mercier J, Leoutsakos J, Madjar C, Lafaille-Magnan ME, Savard M, et al. INTREPAD: a randomized trial of naproxen to slow progress of presymptomatic Alzheimer disease. Neurology. 2019;92:e2070–80.
17. Hershey LA, Lipton RB. Naproxen for presymptomatic Alzheimer disease: is this the end, or shall we try again? Neurology. 2019;92:829–30.
18. Miguel-Alvarez M, Santos-Lozano A, Sanchis-Gomar F, Fiuza-Luces C, Pareja-Galeano H, Garatachea N, et al. Non-steroidal anti-inflammatory drugs as a treatment for Alzheimer's disease: a systematic review and meta-analysis of treatment effect. Drugs Aging. 2015;32:139–47.
19. Ali MM, Ghouri RG, Ans AH, Akbar A, Toheed A. Recommendations for anti-inflammatory treatments in Alzheimer's disease: a Comprehensive Review of the literature. Cureus. 2019;11:e4620.
20. Sochocka M, Diniz BS, Leszek J. Inflammatory response in the CNS: friend or foe? Mol Neurobiol. 2017;54:8071–89.
21. DiSabato DJ, Quan N, Godbout JP. Neuroinflammation: the devil is in the details. J Neurochem. 2016;139(Suppl 2):136–53.
22. Levy BD, Clish CB, Schmidt B, Gronert K, Serhan CN. Lipid mediator class switching during acute inflammation: signals in resolution. Nat Immunol. 2001;2:612–9.
23. Christie WW, Harwood JL. Oxidation of polyunsaturated fatty acids to produce lipid mediators. Essays Biochem. 2020;64:401–21.
24. Wang X, Zhu M, Hjorth E, Cortes-Toro V, Eyjolfsdottir H, Graff C, et al. Resolution of inflammation is altered in Alzheimer's disease. Alzheimers Dement. 2015;11:40–50. e1-2.
25. Zhu M, Wang X, Hjorth E, Colas RA, Schroeder L, Granholm AC, et al. Pro-resolving lipid mediators improve neuronal survival and increase Abeta42 phagocytosis. Mol Neurobiol. 2016;53:2733–49.
26. Do KV, Hjorth E, Wang Y, Jun B, Kautzmann MI, Ohshima M, et al. Cerebrospinal Fluid Profile of lipid mediators in Alzheimer's Disease. Cell Mol Neurobiol. 2023;43:797–811.
27. Lukiw WJ, Cui JG, Marcheselli VL, Bodker M, Botkjaer A, Gotlinger K, et al. A role for docosahexaenoic acid-derived neuroprotectin D1 in neural cell survival and Alzheimer disease. J Clin Invest. 2005;115:2774–83.
28. Bugiani O, Murrell JR, Giaccone G, Hasegawa M, Ghigo G, Tabaton M, et al. Frontotemporal dementia and corticobasal degeneration in a family with a P301S mutation in tau. J Neuropathol Exp Neurol. 1999;58:667–77.
29. Emmerson JT, Do Carmo S, Liu Y, Shalhoub A, Liu A, Bonomo Q, et al. Progressive human-like tauopathy with downstream neurodegeneration and neurovascular compromise in a transgenic rat model. Neurobiol Dis. 2023;184:106227.
30. Emmerson JT, Malcolm JC, Do Carmo S, Nguyen P, Breuillaud L, Martinez-Trujillo JC, et al. Neuronal loss and inflammation preceding fibrillary tau pathology in a rat model with early human-like tauopathy. Neurobiol Dis. 2023;187:106317.
31. Malcolm JC, Breuillaud L, Do Carmo S, Hall H, Welikovitch LA, Macdonald JA, et al. Neuropathological changes and cognitive deficits in rats transgenic for human mutant tau recapitulate human tauopathy. Neurobiol Dis. 2019;127:323–38.
32. Leon WC, Canneva F, Partridge V, Allard S, Ferretti MT, DeWilde A, et al. A novel transgenic rat model with a full Alzheimer's-like amyloid pathology displays pre-plaque intracellular amyloid-beta-associated cognitive impairment. J Alzheimers Dis. 2010;20:113–26.
33. Welikovitch LA, Do Carmo S, Magloczky Z, Malcolm JC, Loke J, Klein WL, et al. Early intraneuronal amyloid triggers neuron-derived inflammatory signaling in APP transgenic rats and human brain. Proc Natl Acad Sci U S A. 2020;117:6844–54.
34. Sosulina L, Mittag M, Geis HR, Hoffmann K, Klyubin I, Qi Y, et al. Hippocampal hyperactivity in a rat model of Alzheimer's disease. J Neurochem. 2021;157:2128–44.
35. Habif M, Do Carmo S, Baez MV, Colettis NC, Cercato MC, Salas DA, et al. Early long-term memory impairment and changes in the expression of synaptic plasticity-Associated genes, in the McGill-R-Thy1-APP rat model of Alzheimer's-Like Brain Amyloidosis. Front Aging Neurosci. 2020;12:585873.
36. Qi Y, Klyubin I, Hu NW, Ondrejcak T, Rowan MJ. Pre-plaque ass-mediated impairment of synaptic depotentiation in a transgenic rat model of Alzheimer's Disease Amyloidosis. Front Neurosci. 2019;13:861.
37. Petrasek T, Vojtechova I, Lobellova V, Popelikova A, Janikova M, Brozka H, et al. The McGill Transgenic Rat Model of Alzheimer's Disease displays Cognitive and Motor impairments, changes in anxiety and Social Behavior, and altered circadian activity. Front Aging Neurosci. 2018;10:250.
38. Parent MJ, Zimmer ER, Shin M, Kang MS, Fonov VS, Mathieu A, et al. Multimodal Imaging in Rat Model recapitulates Alzheimer's disease biomarkers abnormalities. J Neurosci. 2017;37:12263–71.
39. Iulita MF, Bistue Millon MB, Pentz R, Aguilar LF, Do Carmo S, Allard S, et al. Differential deregulation of NGF and BDNF neurotrophins in a transgenic rat model of Alzheimer's disease. Neurobiol Dis. 2017;108:307–23.
40. Do Carmo S, Crynen G, Paradis T, Reed J, Iulita MF, Ducatenzeiler A, et al. Hippocampal proteomic analysis reveals distinct pathway deregulation profiles at early and late stages in a rat model of Alzheimer's-Like amyloid Pathology. Mol Neurobiol. 2018;55:3451–76.
41. Wilson EN, Abela AR, Do Carmo S, Allard S, Marks AR, Welikovitch LA, et al. Intraneuronal amyloid Beta Accumulation disrupts hippocampal CRTC1-Dependent gene expression and cognitive function in a rat model of Alzheimer Disease. Cereb Cortex. 2017;27:1501–11.
42. Heggland I, Storkaas IS, Soligard HT, Kobro-Flatmoen A, Witter MP. Stereological estimation of neuron number and plaque load in the hippocampal region of a transgenic rat model of Alzheimer's disease. Eur J Neurosci. 2015;41:1245–62.
43. Qi Y, Klyubin I, Harney SC, Hu N, Cullen WK, Grant MK, et al. Longitudinal testing of hippocampal plasticity reveals the onset and maintenance of endogenous human ass-induced synaptic dysfunction in individual freely behaving pre-plaque transgenic rats: rapid reversal by anti-ass agents. Acta Neuropathol Commun. 2014;2:175.
44. Nilsen LH, Melo TM, Witter MP, Sonnewald U. Early differences in dorsal hippocampal metabolite levels in males but not females in a transgenic rat model of Alzheimer's disease. Neurochem Res. 2014;39:305–12.

45. Nilsen LH, Witter MP, Sonnewald U. Neuronal and astrocytic metabolism in a transgenic rat model of Alzheimer's disease. J Cereb Blood Flow Metab. 2014;34:906–14.
46. Grant SM, Ducatenzeiler A, Szyf M, Cuello AC. Abeta immunoreactive material is present in several intracellular compartments in transfected, neuronally differentiated, P19 cells expressing the human amyloid beta-protein precursor. J Alzheimers Dis. 2000;2:207–22.
47. Perrot R, Lonchampt P, Peterson AC, Eyer J. Axonal neurofilaments control multiple fiber properties but do not influence structure or spacing of nodes of Ranvier. J Neurosci. 2007;27:9573–84.
48. Perrot R, Berges R, Bocquet A, Eyer J. Review of the multiple aspects of neurofilament functions, and their possible contribution to neurodegeneration. Mol Neurobiol. 2008;38:27–65.
49. Hanzel CE, Pichet-Binette A, Pimentel LS, Iulita MF, Allard S, Ducatenzeiler A, et al. Neuronal driven pre-plaque inflammation in a transgenic rat model of Alzheimer's disease. Neurobiol Aging. 2014;35:2249–62.
50. Harayama T, Shimizu T. Roles of polyunsaturated fatty acids, from mediators to membranes. J Lipid Res. 2020;61:1150–60.
51. Shimizu T. Lipid mediators in health and disease: enzymes and receptors as therapeutic targets for the regulation of immunity and inflammation. Annu Rev Pharmacol Toxicol. 2009;49:123–50.
52. Wang B, Tontonoz P. Phospholipid remodeling in physiology and disease. Annu Rev Physiol. 2019;81:165–88.
53. Antonny B, Vanni S, Shindou H, Ferreira T. From zero to six double bonds: phospholipid unsaturation and organelle function. Trends Cell Biol. 2015;25:427–36.
54. Harayama T, Riezman H. Understanding the diversity of membrane lipid composition. Nat Rev Mol Cell Biol. 2018;19:281–96.
55. Dickson DW, Crystal HA, Mattiace LA, Masur DM, Blau AD, Davies P, et al. Identification of normal and pathological aging in prospectively studied nondemented elderly humans. Neurobiol Aging. 1992;13:179–89.
56. Hanseeuw BJ, Betensky RA, Jacobs HIL, Schultz AP, Sepulcre J, Becker JA, et al. Association of Amyloid and tau with cognition in preclinical Alzheimer Disease: a longitudinal study. JAMA Neurol. 2019;76:915–24.
57. Arboleda-Velasquez JF, Lopera F, O'Hare M, Delgado-Tirado S, Marino C, Chmielewska N, et al. Resistance to autosomal dominant Alzheimer's disease in an APOE3 Christchurch homozygote: a case report. Nat Med. 2019;25:1680–3.
58. Biel D, Brendel M, Rubinski A, Buerger K, Janowitz D, Dichgans M, et al. Tau-PET and in vivo braak-staging as prognostic markers of future cognitive decline in cognitively normal to demented individuals. Alzheimers Res Ther. 2021;13:137.
59. Fleisher AS, Chen K, Quiroz YT, Jakimovich LJ, Gutierrez Gomez M, Langois CM, et al. Associations between biomarkers and age in the presenilin 1 E280A autosomal dominant Alzheimer disease kindred: a cross-sectional study. JAMA Neurol. 2015;72:316–24.
60. Jack CR Jr., Bennett DA, Blennow K, Carrillo MC, Dunn B, Haeberlein SB, et al. NIA-AA Research Framework: toward a biological definition of Alzheimer's disease. Alzheimers Dement. 2018;14:535–62.
61. Jack CR Jr., Knopman DS, Jagust WJ, Petersen RC, Weiner MW, Aisen PS, et al. Tracking pathophysiological processes in Alzheimer's disease: an updated hypothetical model of dynamic biomarkers. Lancet Neurol. 2013;12:207–16.
62. Bennett DA, Schneider JA, Wilson RS, Bienias JL, Arnold SE. Neurofibrillary tangles mediate the association of amyloid load with clinical Alzheimer disease and level of cognitive function. Arch Neurol. 2004;61:378–84.
63. Serrano-Pozo A, Qian J, Muzikansky A, Monsell SE, Montine TJ, Frosch MP, et al. Thal amyloid stages do not significantly Impact the correlation between neuropathological change and cognition in the Alzheimer Disease Continuum. J Neuropathol Exp Neurol. 2016;75:516–26.
64. McDade E, Wang G, Gordon BA, Hassenstab J, Benzinger TLS, Buckles V, et al. Longitudinal cognitive and biomarker changes in dominantly inherited Alzheimer disease. Neurology. 2018;91:e1295–306.
65. Wang L, Benzinger TL, Su Y, Christensen J, Friedrichsen K, Aldea P, et al. Evaluation of tau imaging in staging Alzheimer Disease and revealing interactions between beta-amyloid and Tauopathy. JAMA Neurol. 2016;73:1070–7.
66. Bejanin A, Schonhaut DR, La Joie R, Kramer JH, Baker SL, Sosa N, et al. Tau pathology and neurodegeneration contribute to cognitive impairment in Alzheimer's disease. Brain. 2017;140:3286–300.
67. Saha P, Sen N, Tauopathy. A common mechanism for neurodegeneration and brain aging. Mech Ageing Dev. 2019;178:72–9.
68. Hall B, Mak E, Cervenka S, Aigbirhio FI, Rowe JB, O'Brien JT. In vivo tau PET imaging in dementia: pathophysiology, radiotracer quantification, and a systematic review of clinical findings. Ageing Res Rev. 2017;36:50–63.
69. Yoshiyama Y, Higuchi M, Zhang B, Huang SM, Iwata N, Saido TC, et al. Synapse loss and microglial activation precede tangles in a P301S tauopathy mouse model. Neuron. 2007;53:337–51.
70. Choi YB, Dunn-Meynell AA, Marchese M, Blumberg BM, Gaindh D, Dowling PC, et al. Erythropoietin-derived peptide treatment reduced neurological deficit and neuropathological changes in a mouse model of tauopathy. Alzheimers Res Ther. 2021;13:32.
71. Litvinchuk A, Wan YW, Swartzlander DB, Chen F, Cole A, Propson NE, et al. Complement C3aR inactivation attenuates Tau Pathology and reverses an Immune Network Deregulated in Tauopathy Models and Alzheimer's Disease. Neuron. 2018;100:1337–53. e5.
72. Bussian TJ, Aziz A, Meyer CF, Swenson BL, van Deursen JM, Baker DJ. Clearance of senescent glial cells prevents tau-dependent pathology and cognitive decline. Nature. 2018;562:578–82.
73. Belkhelfa M, Rafa H, Medjeber O, Arroul-Lammali A, Behairi N, Abada-Bendib M, et al. IFN-gamma and TNF-alpha are involved during Alzheimer disease progression and correlate with nitric oxide production: a study in Algerian patients. J Interferon Cytokine Res. 2014;34:839–47.
74. Cuello AC, Ferretti MT, Iulita MF. Preplaque ('preclinical') abeta-induced inflammation and nerve growth factor deregulation in transgenic models of Alzheimer's disease-like amyloid pathology. Neurodegener Dis. 2012;10:104–7.
75. Ferretti MT, Bruno MA, Ducatenzeiler A, Klein WL, Cuello AC. Intracellular abeta-oligomers and early inflammation in a model of Alzheimer's disease. Neurobiol Aging. 2012;33:1329–42.
76. Lambert MP, Velasco PT, Chang L, Viola KL, Fernandez S, Lacor PN, et al. Monoclonal antibodies that target pathological assemblies of Abeta. J Neurochem. 2007;100:23–35.
77. Ricciotti E, FitzGerald GA. Prostaglandins and inflammation. Arterioscler Thromb Vasc Biol. 2011;31:986–1000.
78. Chen C, Bazan NG. Endogenous PGE2 regulates membrane excitability and synaptic transmission in hippocampal CA1 pyramidal neurons. J Neurophysiol. 2005;93:929–41.
79. Chen C, Magee JC, Bazan NG. Cyclooxygenase-2 regulates prostaglandin E2 signaling in hippocampal long-term synaptic plasticity. J Neurophysiol. 2002;87:2851–7.
80. Tachikawa M, Hosoya K, Terasaki T. Pharmacological significance of prostaglandin E2 and D2 transport at the brain barriers. Adv Pharmacol. 2014;71:337–60.
81. Hein AM, Stutzman DL, Bland ST, Barrientos RM, Watkins LR, Rudy JW, et al. Prostaglandins are necessary and sufficient to induce contextual fear learning impairments after interleukin-1 beta injections into the dorsal hippocampus. Neuroscience. 2007;150:754–63.
82. Matsumoto Y, Yamaguchi T, Watanabe S, Yamamoto T. Involvement of arachidonic acid cascade in working memory impairment induced by interleukin-1 beta. Neuropharmacology. 2004;46:1195–200.
83. Minhas PS, Latif-Hernandez A, McReynolds MR, Durairaj AS, Wang Q, Rubin A, et al. Restoring metabolism of myeloid cells reverses cognitive decline in ageing. Nature. 2021;590:122–8.
84. Lalier L, Cartron PF, Olivier C, Loge C, Bougras G, Robert JM, et al. Prostaglandins antagonistically control Bax activation during apoptosis. Cell Death Differ. 2011;18:528–37.
85. Iwasa K, Yamamoto S, Yagishita S, Maruyama K, Yoshikawa K. Excitotoxicity-induced prostaglandin D(2) production induces sustained microglial activation and delayed neuronal death. J Lipid Res. 2017;58:649–55.
86. Yoshikawa K, Kita Y, Furukawa A, Kawamura N, Hasegawa-Ishii S, Chiba Y, et al. Excitotoxicity-induced immediate surge in hippocampal prostanoid production has latent effects that promote chronic progressive neuronal death. Prostaglandins Leukot Essent Fat Acids. 2013;88:373–81.
87. Bilak M, Wu L, Wang Q, Haughey N, Conant K, St Hillaire C, et al. PGE2 receptors rescue motor neurons in a model of amyotrophic lateral sclerosis. Ann Neurol. 2004;56:240–8.
88. Loynes CA, Lee JA, Robertson AL, Steel MJ, Ellett F, Feng Y, et al. PGE(2) production at sites of tissue injury promotes an anti-inflammatory neutrophil phenotype and determines the outcome of inflammation resolution in vivo. Sci Adv. 2018;4:eaar8320.
89. Andreasson K. Emerging roles of PGE2 receptors in models of neurological disease. Prostaglandins Other Lipid Mediat. 2010;91:104–12.

90. Bazan NG, Colangelo V, Lukiw WJ. Prostaglandins and other lipid mediators in Alzheimer's disease. Prostaglandins Other Lipid Mediat. 2002;68–69:197–210.
91. Figueiredo-Pereira ME, Corwin C, Babich J. Prostaglandin J2: a potential target for halting inflammation-induced neurodegeneration. Ann N Y Acad Sci. 2016;1363:125–37.
92. Johansson JU, Woodling NS, Wang Q, Panchal M, Liang X, Trueba-Saiz A, et al. Prostaglandin signaling suppresses beneficial microglial function in Alzheimer's disease models. J Clin Invest. 2015;125:350–64.
93. Liang X, Wu L, Hand T, Andreasson K. Prostaglandin D2 mediates neuronal protection via the DP1 receptor. J Neurochem. 2005;92:477–86.
94. Shi J, Wang Q, Johansson JU, Liang X, Woodling NS, Priyam P, et al. Inflammatory prostaglandin E2 signaling in a mouse model of Alzheimer disease. Ann Neurol. 2012;72:788–98.
95. Wei LL, Shen YD, Zhang YC, Hu XY, Lu PL, Wang L, et al. Roles of the prostaglandin E2 receptors EP subtypes in Alzheimer's disease. Neurosci Bull. 2010;26:77–84.
96. Wood H. Alzheimer disease: prostaglandin E(2) signalling is implicated in inflammation early in the Alzheimer disease course. Nat Rev Neurol. 2012;8:411.
97. Woodling NS, Andreasson KI. Untangling the web: toxic and protective effects of Neuroinflammation and PGE2 Signaling in Alzheimer's Disease. ACS Chem Neurosci. 2016;7:454–63.
98. Nishida N, Nagata N, Toda H, Jingami N, Uemura K, Ozaki A, et al. Association of lipocalin-type prostaglandin D synthase with disproportionately enlarged subarachnoid-space in idiopathic normal pressure hydrocephalus. Fluids Barriers CNS. 2014;11:9.
99. Kanekiyo T, Ban T, Aritake K, Huang ZL, Qu WM, Okazaki I, et al. Lipocalin-type prostaglandin D synthase/beta-trace is a major amyloid beta-chaperone in human cerebrospinal fluid. Proc Natl Acad Sci U S A. 2007;104:6412–7.
100. Hoshino T, Namba T, Takehara M, Murao N, Matsushima T, Sugimoto Y, et al. Improvement of cognitive function in Alzheimer's disease model mice by genetic and pharmacological inhibition of the EP(4) receptor. J Neurochem. 2012;120:795–805.
101. Akitake Y, Nakatani Y, Kamei D, Hosokawa M, Akatsu H, Uematsu S, et al. Microsomal prostaglandin E synthase-1 is induced in alzheimer's disease and its deletion mitigates alzheimer's disease-like pathology in a mouse model. J Neurosci Res. 2013;91:909–19.
102. Emre C, Do KV, Jun B, Hjorth E, Alcalde SG, Kautzmann MI, et al. Age-related changes in brain phospholipids and bioactive lipids in the APP knock-in mouse model of Alzheimer's disease. Acta Neuropathol Commun. 2021;9:116.
103. Sanchez-Mejia RO, Mucke L. Phospholipase A2 and arachidonic acid in Alzheimer's disease. Biochim Biophys Acta. 2010;1801:784–90.
104. Sanchez-Mejia RO, Newman JW, Toh S, Yu GQ, Zhou Y, Halabisky B, et al. Phospholipase A2 reduction ameliorates cognitive deficits in a mouse model of Alzheimer's disease. Nat Neurosci. 2008;11:1311–8.
105. Wang Y, Guan PP, Yu X, Guo YS, Zhang YJ, Wang ZY, et al. COX-2 metabolic products, the prostaglandin I(2) and F(2alpha), mediate the effects of TNF-alpha and zn(2+) in stimulating the phosphorylation of tau. Oncotarget. 2017;8:99296–311.
106. Arnaud LT, Myeku N, Figueiredo-Pereira ME. Proteasome-caspase-cathepsin sequence leading to tau pathology induced by prostaglandin J2 in neuronal cells. J Neurochem. 2009;110:328–42.
107. Bitto A, Giuliani D, Pallio G, Irrera N, Vandini E, Canalini F, et al. Effects of COX1-2/5-LOX blockade in Alzheimer transgenic 3xTg-AD mice. Inflamm Res. 2017;66:389–98.
108. Bazan NG. COX-2 as a multifunctional neuronal modulator. Nat Med. 2001;7:414–5.
109. Bellucci A, Westwood AJ, Ingram E, Casamenti F, Goedert M, Spillantini MG. Induction of inflammatory mediators and microglial activation in mice transgenic for mutant human P301S tau protein. Am J Pathol. 2004;165:1643–52.
110. Oka A, Takashima S. Induction of cyclo-oxygenase 2 in brains of patients with Down's syndrome and dementia of Alzheimer type: specific localization in affected neurones and axons. NeuroReport. 1997;8:1161–4.
111. Molina-Holgado E, Ortiz S, Molina-Holgado F, Guaza C. Induction of COX-2 and PGE(2) biosynthesis by IL-1beta is mediated by PKC and mitogen-activated protein kinases in murine astrocytes. Br J Pharmacol. 2000;131:152–9.
112. Lukiw WJ, Mukherjee PK, Cui JG, Bazan NG. A2E selectively induces cox-2 in ARPE-19 and human neural cells. Curr Eye Res. 2006;31:259–63.
113. Amadoro G, Ciotti MT, Costanzi M, Cestari V, Calissano P, Canu N. NMDA receptor mediates tau-induced neurotoxicity by calpain and ERK/MAPK activation. Proc Natl Acad Sci U S A. 2006;103:2892–7.
114. Stark DT, Bazan NG. Synaptic and extrasynaptic NMDA receptors differentially modulate neuronal cyclooxygenase-2 function, lipid peroxidation, and neuroprotection. J Neurosci. 2011;31:13710–21.
115. Zhao Y, Calon F, Julien C, Winkler JW, Petasis NA, Lukiw WJ, et al. Docosahexaenoic acid-derived neuroprotectin D1 induces neuronal survival via secretase- and PPARgamma-mediated mechanisms in Alzheimer's disease models. PLoS ONE. 2011;6:e15816.
116. Mizwicki MT, Liu G, Fiala M, Magpantay L, Sayre J, Siani A, et al. 1alpha,25-dihydroxyvitamin D3 and resolvin D1 retune the balance between amyloid-beta phagocytosis and inflammation in Alzheimer's disease patients. J Alzheimers Dis. 2013;34:155–70.
117. Fiala M, Terrando N, Dalli J. Specialized Pro-resolving mediators from Omega-3 fatty acids improve amyloid-beta phagocytosis and regulate inflammation in patients with minor cognitive impairment. J Alzheimers Dis. 2016;49:1191.
118. Li C, Wu X, Liu S, Shen D, Zhu J, Liu K. Role of Resolvins in the Inflammatory Resolution of Neurological diseases. Front Pharmacol. 2020;11:612.
119. Kantarci A, Aytan N, Palaska I, Stephens D, Crabtree L, Benincasa C, et al. Combined administration of resolvin E1 and lipoxin A4 resolves inflammation in a murine model of Alzheimer's disease. Exp Neurol. 2018;300:111–20.
120. Bazan NG. Homeostatic regulation of photoreceptor cell integrity: significance of the potent mediator neuroprotectin D1 biosynthesized from docosahexaenoic acid: the Proctor Lecture. Invest Ophthalmol Vis Sci. 2007;48:4866-81; biography 4–5.
121. Stark DT, Bazan NG. Neuroprotectin D1 induces neuronal survival and downregulation of amyloidogenic processing in Alzheimer's disease cellular models. Mol Neurobiol. 2011;43:131–8.
122. Calandria JM, Sharp MW, Bazan NG. The Docosanoid Neuroprotectin D1 induces TH-Positive neuronal survival in a Cellular Model of Parkinson's Disease. Cell Mol Neurobiol. 2015;35:1127–36.
123. Calandria JM, Asatryan A, Balaszczuk V, Knott EJ, Jun BK, Mukherjee PK, et al. NPD1-mediated stereoselective regulation of BIRC3 expression through cREL is decisive for neural cell survival. Cell Death Differ. 2015;22:1363–77.
124. Pham TL, Kakazu AH, He J, Nshimiyimana R, Petasis NA, Jun B, et al. Elucidating the structure and functions of Resolvin D6 isomers on nerve regeneration with a distinctive trigeminal transcriptome. FASEB J. 2021;35:e21775.
125. Bhattacharjee S, Jun B, Belayev L, Heap J, Kautzmann MA, Obenaus A, et al. Elovanoids are a novel class of homeostatic lipid mediators that protect neural cell integrity upon injury. Sci Adv. 2017;3:e1700735.
126. Bazan NG. Overview of how N32 and N34 elovanoids sustain sight by protecting retinal pigment epithelial cells and photoreceptors. J Lipid Res. 2021;62:100058.
127. Yeboah GK, Lobanova ES, Brush RS, Agbaga MP. Very long chain fatty acid-containing lipids: a decade of novel insights from the study of ELOVL4. J Lipid Res. 2021;62:100030.
128. Calandria JM, Bhattacharjee S, Maness NJ, Kautzmann MI, Asatryan A, Gordon WC, et al. Elovanoids Downregulate SARS-CoV-2 cell-entry, canonical mediators and enhance protective signaling in human alveolar cells. Sci Rep. 2021;11:12324.
129. Resano A, Bhattacharjee S, Barajas M, Do KV, Aguado-Jimenez R, Rodriguez D et al. Elovanoids Counteract Inflammatory Signaling, Autophagy, endoplasmic reticulum stress, and Senescence Gene Programming in Human nasal epithelial cells exposed to Allergens. Pharmaceutics. 2022;14.
130. Dyall SC, Balas L, Bazan NG, Brenna JT, Chiang N, da Costa Souza F, et al. Polyunsaturated fatty acids and fatty acid-derived lipid mediators: recent advances in the understanding of their biosynthesis, structures, and functions. Prog Lipid Res. 2022;86:101165.
131. Bazan NG. Docosanoids and elovanoids from omega-3 fatty acids are pro-homeostatic modulators of inflammatory responses, cell damage and neuroprotection. Mol Aspects Med. 2018;64:18–33.
132. Lauwers E, Goodchild R, Verstreken P. Membrane lipids in presynaptic function and disease. Neuron. 2016;90:11–25.
133. Hopiavuori BR, Deak F, Wilkerson JL, Brush RS, Rocha-Hopiavuori NA, Hopiavuori AR, et al. Homozygous expression of mutant ELOVL4 leads to seizures and death in a Novel Animal Model of very long-chain fatty acid Deficiency. Mol Neurobiol. 2018;55:1795–813.
134. Suh M, Wierzbicki AA, Lien EL, Clandinin MT. Dietary 20:4n-6 and 22:6n-3 modulates the profile of long- and very-long-chain fatty acids, rhodopsin content, and kinetics in developing photoreceptor cells. Pediatr Res. 2000;48:524–30.
135. Suh M, Sauve Y, Merrells KJ, Kang JX, Ma DW. Supranormal electroretinogram in fat-1 mice with retinas enriched in docosahexaenoic acid

and n-3 very long chain fatty acids (C24-C36). Invest Ophthalmol Vis Sci. 2009;50:4394–401.
136. Agbaga MP, Mandal MN, Anderson RE. Retinal very long-chain PUFAs: new insights from studies on ELOVL4 protein. J Lipid Res. 2010;51:1624–42.
137. Cheng V, Rallabandi R, Gorusupudi A, Lucas S, Rognon G, Bernstein PS, et al. Influence of very-long-chain polyunsaturated fatty acids on membrane structure and dynamics. Biophys J. 2022;121:2730–41.
138. Aveldano MI. Long and very long polyunsaturated fatty acids of retina and spermatozoa: the whole complement of polyenoic fatty acid series. Adv Exp Med Biol. 1992;318:231–42.
139. Poulos A, Sharp P, Singh H, Johnson D, Fellenberg A, Pollard A. Detection of a homologous series of C26-C38 polyenoic fatty acids in the brain of patients without peroxisomes (Zellweger's syndrome). Biochem J. 1986;235:607–10.
140. Schonfeld P, Reiser G. Brain lipotoxicity of Phytanic Acid and very long-chain fatty acids. Harmful Cellular/Mitochondrial activities in Refsum Disease and X-Linked Adrenoleukodystrophy. Aging Dis. 2016;7:136–49.
141. Wanders RJ. Metabolic functions of peroxisomes in health and disease. Biochimie. 2014;98:36–44.
142. Wood PL. Lipidomics of Alzheimer's disease: current status. Alzheimers Res Ther. 2012;4:5.
143. Kou J, Kovacs GG, Hoftberger R, Kulik W, Brodde A, Forss-Petter S, et al. Peroxisomal alterations in Alzheimer's disease. Acta Neuropathol. 2011;122:271–83.
144. Do KV, Kautzmann MI, Jun B, Gordon WC, Nshimiyimana R, Yang R, et al. Elovanoids counteract oligomeric beta-amyloid-induced gene expression and protect photoreceptors. Proc Natl Acad Sci U S A. 2019;116:24317–25.
145. He Y, Phan K, Bhatia S, Pickford R, Fu Y, Yang Y, et al. Increased VLCFA-lipids and ELOVL4 underlie neurodegeneration in frontotemporal dementia. Sci Rep. 2021;11:21348.
146. Han X, D MH, McKeel DW Jr., Kelley J, Morris JC. Substantial sulfatide deficiency and ceramide elevation in very early Alzheimer's disease: potential role in disease pathogenesis. J Neurochem. 2002;82:809–18.
147. Han X, Holtzman DM, McKeel DW. Jr. Plasmalogen deficiency in early Alzheimer's disease subjects and in animal models: molecular characterization using electrospray ionization mass spectrometry. J Neurochem. 2001;77:1168–80.
148. Kosicek M, Hecimovic S. Phospholipids and Alzheimer's disease: alterations, mechanisms and potential biomarkers. Int J Mol Sci. 2013;14:1310–22.
149. Obis E, Sol J, Andres-Benito P, Martin-Gari M, Mota-Martorell N, Galo-Licona JD, et al. Lipidomic alterations in the Cerebral Cortex and White Matter in sporadic Alzheimer's Disease. Aging Dis. 2023;14:1887–916.
150. Bok E, Leem E, Lee BR, Lee JM, Yoo CJ, Lee EM, et al. Role of the Lipid Membrane and Membrane Proteins in Tau Pathology. Front Cell Dev Biol. 2021;9:653815.
151. El Mammeri N, Gampp O, Duan P, Hong M. Membrane-induced tau amyloid fibrils. Commun Biol. 2023;6:467.
152. Sallaberry CA, Voss BJ, Majewski J, Biernat J, Mandelkow E, Chi EY, et al. Tau and membranes: interactions that promote folding and condensation. Front Cell Dev Biol. 2021;9:725241.
153. Ait-Bouziad N, Lv G, Mahul-Mellier AL, Xiao S, Zorludemir G, Eliezer D, et al. Discovery and characterization of stable and toxic Tau/phospholipid oligomeric complexes. Nat Commun. 2017;8:1678.
154. Fanni AM, Vander Zanden CM, Majewska PV, Majewski J, Chi EY. Membrane-mediated fibrillation and toxicity of the tau hexapeptide PHF6. J Biol Chem. 2019;294:15304–17.
155. Chang CC, Edwald E, Veatch S, Steel DG, Gafni A. Interactions of amyloid-beta peptides on lipid bilayer studied by single molecule imaging and tracking. Biochim Biophys Acta Biomembr. 2018;1860:1616–24.
156. Meker S, Chin H, Sut TN, Cho NJ. Amyloid-beta peptide triggers membrane remodeling in supported lipid bilayers depending on their hydrophobic thickness. Langmuir. 2018;34:9548–60.
157. Wiatrak B, Piasny J, Kuzniarski A, Gasiorowski K. Interactions of amyloid-beta with membrane proteins. Int J Mol Sci. 2021;22.

Publisher's Note